

000 001 002 003 004 005 006 007 ALIGNING FROZEN LLMS BY REINFORCEMENT 008 LEARNING: AN ITERATIVE REWEIGHT-THEN- 009 OPTIMIZE APPROACH 010 011 012

013 **Anonymous authors**
014 **Paper under double-blind review**
015
016
017
018
019
020
021
022
023
024
025
026
027
028
029
030
031
032
033
034
035
036
037

ABSTRACT

038 Aligning large language models (LLMs) with human preferences usually requires
039 fine-tuning methods such as RLHF and DPO. These methods directly optimize
040 the model parameters, so they cannot be used in inference time to improve model
041 performance, nor are they applicable when the model weights are not accessible.
042 In contrast, inference-time methods sidestep weight updates by leveraging reward
043 functions to guide and improve output quality. However, they incur high inference
044 costs, and their one-shot guidance is often based on imperfect reward or value
045 functions, leading to suboptimal outputs. In this work, we present a method named
046 Iterative Reweight-then-Optimize (IRO), a reinforcement learning (RL) framework
047 that performs RL-style alignment of the (frozen) base model without touching
048 its parameters. During training, each iteration (*i*) samples candidates from the
049 base model, (*ii*) resamples using current value functions, and (*iii*) trains a new
050 lightweight value function that guides the next decoding pass. At inference time,
051 the value functions are used to guide the base model generation via a search-based
052 optimization process. We prove that under some mild conditions, IRO is a kind
053 of policy iteration and attains the performance of Best-of-N (BoN) search with
054 exponentially fewer tokens at inference time. Experimental results demonstrate that
055 IRO significantly improves length-controlled win rates on challenging instruction-
056 following benchmarks, such as AlpacaEval 2.0, achieving a substantial performance
057 boost (e.g., 30.71% \rightarrow 43.80% for Llama-3-8B-Instruct and 43.11% \rightarrow
058 49.77% for Llama-3-70B-Instruct compared against GPT-4 responses).
059 Further, IRO consistently outperforms SOTA inference-time alignment baselines
060 such as BoN and weak-to-strong search, even when using much smaller value
061 functions (of size 1B or 7B) to guide a large base model (of size 6.9B or 70B).
062 **Moreover, we demonstrate that multiple value functions can be compressed into a**
063 **single lightweight value function, substantially reducing memory usage and latency**
064 **while preserving competitive performance.**

065 1 INTRODUCTION

066 Large Language Models (LLMs) have demonstrated impressive capabilities across tasks such as
067 AI assistance (Achiam et al., 2023; Guo et al., 2025) and multi-step reasoning (Bai et al., 2023).
068 To align model behavior with human preferences, most existing approaches rely on training-time
069 techniques, notably Reinforcement Learning with Human Feedback (RLHF) (Ouyang et al., 2022)
070 and Direct Preference Optimization (DPO) (Rafailov et al., 2024b). These methods require access to
071 model parameters and perform direct weight updates using human-labeled data or preference-derived
072 rewards. While effective, such approaches suffer from a fundamental limitation, **that they cannot**
073 **be applied to further improve model performance or adapt to new domains at inference time.**
074 Indeed, once a model is frozen or deployed, these methods offer no means of further fine-tuning
075 based on downstream user feedback or new reward signals. Any significant shift in user preferences
076 or application context typically necessitates costly re-optimization. These limitations are especially
077 problematic in real-world deployment settings where models must quickly adapt to new instructions,
078 tasks, or evaluation objectives without retraining. For instance, a safety-tuned model may require
079 reward-specific customization depending on user goals. In response, there has been growing interest

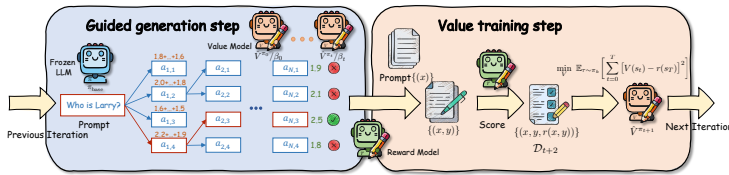


Figure 1: Illustration of the proposed Iterative Reweighting-and-Optimization (IRO). It consists of two steps: (1) Guided generation step: candidate sequences are first sampled from the base model, then reweighted based on scores from value functions, and finally selected using a reward model. (2) Value training step: a reward model scores the generated sample, and a new lightweight value function is trained via regression. At inference time, the trained value functions are used to guide generation.

in **inference-time alignment methods** (Snell et al., 2024; Mudgal et al., 2023; Xu et al., 2024b), which aim to improve generation quality by leveraging external guidance—such as reward or value functions—without modifying the underlying model weights.

Most inference-time methods assume access to an outcome reward model (ORM), which evaluates the quality of a complete output. ORMs are extremely popular in practice partly because they are relatively easy to obtain: they can be trained using standard preference data or derived from existing evaluation pipelines (e.g., through GPT-4 comparisons, rubric scoring, or upvote logs) (Zhu et al., 2023; Jiang et al., 2023). However, ORM-based inference-time alignment methods face a key trade-off between granularity and efficiency: response-level scoring (such as the popular Best-of- N (BoN) (Nakano et al., 2021; Stiennon et al., 2020)) is coarse and costly and requires a large number of generations to match training-time performance (Gao et al., 2023; Dubois et al., 2023). Methods based on token-level scoring are either inaccurate (such as ARGs (Khanov et al., 2024), which constructs a token-level score function by applying the ORM to partial generations) or computationally intensive (requires full-continuation rollouts (Chakraborty et al., 2024; Huang et al., 2024a)).

Alternatively, one can train an external value function, sometimes also called a process reward model (PRM) to guide generation (Mudgal et al., 2023; Han et al., 2024; Kong et al., 2024). These methods provide finer-grained guidance but face two key limitations: (1) high cost or inaccessibility of training supervision (e.g., OpenAI’s PRM800K dataset (Lightman et al., 2023) was constructed through extensive manual annotation of intermediate reasoning steps), and (2) inability to correct or refine model behavior over multiple inference steps, i.e., value functions are used to rescore or filter outputs in a single pass, resulting in suboptimal outputs, especially in challenging or long-horizon tasks. For more detailed discussion of ORM and value function/PRM based methods, we defer to Appendix A.

Research Question, Proposed Work and Contributions. Based on the above discussion, this work focuses on addressing the following key research question:

Given access to a frozen LLM and an ORM, how can we best improve or customize the model at inference time, while minimizing inference-time inference cost?

In this paper, we propose Iterative Reweighting-and-Optimization (IRO), a Reinforcement Learning (RL) inspired framework that performs RL-style alignment for the (frozen) base model without touching its parameters. Unlike most existing inference-time alignment approaches, which apply a one-shot improvement, our framework enables successive policy improvement by applying a *sequence* of value functions, trained iteratively via the following three key steps: (i) samples candidates from the base model, (ii) resamples using current value functions, and (iii) trains a new lightweight value function that guides the next decoding pass. At inference time, the sequence of learned value functions is then applied to guide the base model generation via a search-based optimization process. **We further show that these multiple value functions can be compressed into a single lightweight value function, substantially reducing memory usage and latency while preserving competitive performance.** It is worth mentioning that users can use the proposed IRO to finetune a model on their own dataset in the RL style, following a similar procedure to OpenAI’s reinforcement fine-tuning (RFT), but without needing to access the model weights. Please see Fig. 1 for an illustration of the proposed scheme. There are a number of major advantages of the proposed approach compared with the existing approaches mentioned above.

108 (1). Compared with ORM-based and approaches such as ARGS (Khanov et al., 2024) and PRM-
 109 based methods (Lightman et al., 2023; Cheng et al., 2025), IRO provides an efficient, fine-grained
 110 *token-level* guidance without requiring step-level annotations, guiding the *frozen model* generation
 111 towards much higher quality.

112 (2). Unlike most existing methods providing one-shot guidance, IRO enables *multi-iteration* policy
 113 improvement by employing lightweight, iteratively trained value functions to approximate iterative
 114 policy improvement in the frozen-model setting.

115 (3). Compared with the popular baseline BoN, our approach is significantly more computationally
 116 efficient at inference time, and attains the performance of BoN with exponentially fewer tokens.

117 Our specific technical contributions can be summarized as follows:

118 (1) To begin with, we made a key observation that finding the optimal alignment policy is equivalent to
 119 finding a sequence of value functions, each solving a constrained policy optimization problem. Based
 120 on this, we design a novel IRO approach on reweighting self-generated data to enable *successive*
 121 policy improvement, which theoretically converges to the optimal policy. Furthermore, we prove that
 122 under some ideal conditions, IRO achieves the same performance as BoN (i.e., the same probability
 123 of identifying the optimal generation), but requires *exponentially fewer* tokens and external queries.

124 (2) Empirically, we provide extensive evidence demonstrating that IRO significantly improves
 125 over existing inference-time alignment methods. For instance, IRO improves length-controlled
 126 win rates on instruction-following benchmarks AlpacaEval 2.0 compared with the frozen base
 127 model (e.g., 30.71% \rightarrow 43.11% for Llama-3-8B-Instruct and 43.11% \rightarrow 49.77% for
 128 Llama-3-70B-Instruct compared against GPT-4 responses). Further, IRO consistently outper-
 129 forms SOTA inference-time alignment baselines such as BoN and weak-to-strong-search, even when
 130 using much smaller value functions (of size 1B or 7B) to guide large base models (6.9B or 70B).
 131 Additionally, extensive ablation studies have been done to analyze the impact of key algorithmic
 132 choices and robustness under imperfect reward models.

133 (3) Although IRO involves multiple value functions at inference-time, we further show that they can
 134 be compressed into a single value function. This compression significantly reduces 18-45% memory
 135 cost and 24-40% latency while only drop 0-1.7% win rates performance compared with IRO Iter3.

136 Overall, our method proposed a novel framework to achieve RL-style alignment on a frozen base
 137 LLM, enabling multi-iteration policy improvement during inference time. Moreover, we also show
 138 that, under some standard assumptions, the proposed method is theoretically equivalent to an RL-
 139 based policy optimization algorithm, and that it can be exponentially more efficient than the standard
 140 inference-time approaches such as BoN.

2 PRELIMINARIES AND PROBLEM FORMULATION

2.1 NOTATIONS AND PRELIMINARIES

141 **The Finite-Horizon MDP Model.** A finite Markov decision process (MDP) is defined by the
 142 tuple $(\mathcal{S}, \mathcal{A}, \mathcal{P}, \mu, r, H)$, where $\mathcal{S} = \{\mathcal{S}_h\}_{h=1}^H$ is the state space, \mathcal{A} the action space, \mathcal{P} the
 143 transition dynamics, $\mu(\cdot)$ the initial state distribution, r the reward function, and H the horizon.
 144 A trajectory is denoted as $\tau := (s_1, a_1, s_2, \dots, s_H, a_H)$. Further define the corresponding state-
 145 action visitation measure as $d_h^\pi(s, a) := \mathbb{E}_{s_1 \sim \mu} [\mathcal{P}^\pi(s_h = s, a_h = a | s_1)]$, and state visitation
 146 measures as $d_h^\pi(s) := \sum_{a \in \mathcal{A}} d_h^\pi(s, a)$. The value functions and Q functions under policy π as
 147 $V^\pi(s) := \mathbb{E}_{\tau \sim \pi} \left[\sum_{i=h}^H r(s_i, a_i) \mid s_h = s \right]$, $Q^\pi(s, a) := \mathbb{E}_{\tau \sim \pi} \left[\sum_{i=h}^H r(s_i, a_i) \mid s_h = s, a_h = a \right]$
 148 for all $s_h \in \mathcal{S}_h, a \in \mathcal{A}$, and the advantage function is given by $A^\pi(s_h, a_h) := Q^\pi(s_h, a_h) - V^\pi(s_h)$.

149 **Token-level MDP Model of LLM.** The text generation process of LLM can be modeled as an episodic
 150 time-inhomogeneous MDP. Denote the prompt as x and output continuation as $y := (y_1, \dots, y_H)$ with
 151 maximum length H . At each timestep h , the state is $s_h := [x, y_{1:h-1}]$, including the prompt and the
 152 generated prefix, while the action $a_h = y_h$ is the next token. Since each state s_h encodes a unique
 153 prefix, the state spaces $\{\mathcal{S}_h\}_{h=1}^H$ are mutually disjoint. The transition kernel \mathcal{P} is deterministic, i.e.
 154 given state s_h and action a_h , $s_{h+1} = \mathcal{P}(s_h, a_h) = [s_h, a_h]$. With an outcome reward (ORM), the
 155 reward is given only at the end of the generation Ouyang et al. (2022), i.e., $r(s_h, a_h) = 0$ for all
 156 $h < H$, and $r(s_H, a_H) = r(\tau)$ where $r(\tau)$ is the reward for the entire sequence τ . For simplicity,
 157 we sometimes refer to both $Q^\pi(s_h, a_h)$ and $V^\pi(s_h)$ as the value function.

162 **Policy Optimization.** Using the above notations, the policy optimization problem is given by
 163

$$164 \quad \max_{\pi} J(\pi) := \max_{\pi} \mathbb{E}_{s_1 \sim \mu, \tau \sim \pi} r(\tau), \quad (1)$$

165 where $\tau := (s_1, a_1, s_2, a_2, \dots)$ denotes one trajectory, corresponding to one data point with prompt(s)
 166 and continuation(s). The goal is to find the optimal policy as $\pi^* = \arg \max_{\pi} J(\pi)$. The optimal
 167 value function is defined as $V^*(s_h) = \mathbb{E}_{\tau \sim \pi^*} \left[\sum_{i=h}^H r(s_i, a_i) | s_h \right]$.
 168

169 Since this work focuses on fine-tuning a base model, the above policy optimization problem is
 170 conducted on top of a base model, denoted as π_{base} . Then problem (1) is equivalent to maximizing
 171 the following performance gap:
 172

$$173 \quad \eta^{\pi_{\text{base}}}(\pi) := J(\pi) - J(\pi_{\text{base}}) \stackrel{(i)}{=} \sum_{h=1}^H \mathbb{E}_{s_h \sim d_h^{\pi}, a_h \sim \pi(\cdot | s)} [A^{\pi_{\text{base}}}(s_h, a_h)], \quad (2)$$

175 where (i) is due to the performance difference lemma (see Lemma 1 in the appendix). Thus, the
 176 policy optimization problem reduces to seeking a policy π that induces maximum expected advantage
 177 with respect to the base policy π_{base} under its visitation state distribution d_h^{π} .
 178

179 2.2 POLICY OPTIMIZATION VIA LEARNING A SEQUENCE OF VALUE FUNCTIONS.

180 To maximize the performance gap, we can directly optimize (2). However, it is required to sample the
 181 data from the visitation measure $d_h^{\pi}(\cdot)$, which is infeasible in practice. To address this, we follow the
 182 trust region policy optimization (TRPO, see Schulman (2015)), which constructs a more conservative
 183 but easy surrogate for the performance gap, and successively optimizes it. Assume that we want to
 184 improve a *reference* policy π' (not necessarily π_{base}). Consider the following surrogate objective:
 185

$$186 \quad \tilde{\eta}^{\pi'}(\pi) = \sum_{h=1}^H \mathbb{E}_{s_h \sim d_h^{\pi'}, a_h \sim \pi(\cdot | s)} [A^{\pi'}(s_h, a_h)]. \quad (3)$$

188 Note that s_h is sampled from the visitation measure of the reference model, which is easier to obtain.
 189 $\tilde{\eta}^{\pi'}(\pi)$ serves as a good approximation to $\eta^{\pi'}(\pi)$ (i.e., $\eta^{\pi_{\text{base}}}(\pi)$ in (2) with π_{base} replaced by π')
 190 when π and π' are close in terms of the KL-divergence. Thus, one can instead maximize the surrogate
 191 objective $\tilde{\eta}^{\pi'}(\pi)$ while penalizing the KL divergence between π and π' . This naturally leads to
 192 a KL-constrained optimization problem, which guarantees monotonic performance improvement
 193 at each iteration (Shani et al., 2020; Schulman, 2015). The objective is to maximize a surrogate
 194 performance difference while limiting deviation from a reference policy π' :
 195

$$196 \quad \max_{\pi} \tilde{\eta}^{\pi'}(\pi) \quad (4a)$$

$$197 \quad \text{s.t.} \quad \sum_{h=1}^H \mathbb{E}_{s_h \sim d_h^{\pi'}} [D_{\text{KL}}(\pi(\cdot | s_h) || \pi'(\cdot | s_h))] \leq \epsilon, \quad \pi(\cdot | s_h) \in \Delta_{\mathcal{A}}, \quad \forall h \in [H], \quad (4b)$$

199 where $\Delta_{\mathcal{A}}$ is the probability simplex on the action space. Solving the above KL-constrained problem
 200 (4) yields the following closed-form update for each $h \in [H]$ (Schulman, 2015; Zhang et al., 2024)
 201 (See Appendix B.1):
 202

$$203 \quad \pi_{\text{new}}(a_h | s_h) \propto \pi'(a_h | s_h) \exp \left(\frac{1}{\beta} Q^{\pi'}(s_h, a_h) \right) = \pi'(a_h | s_h) \exp \left(\frac{1}{\beta} V^{\pi'}(s_{h+1}) \right), \quad (5)$$

204 where β is the dual variables of the KL constraints, and $Q^{\pi'}$ is the Q function for the reference
 205 policy; the last equality is due to the equivalence between V and Q mentioned before. This update
 206 softly reweights the reference policy based on the estimated value function. The parameter β serves a
 207 critical role that regulates exploration and exploitation: large β yields conservative steps close to π' ,
 208 while small β allows more aggressive exploitation of the value estimates. A *key insight* from (5) is
 209 that the policy updates depend only on the current policy's value function.
 210

211 Of course, since (3) is an approximation of the performance gap, optimizing it does not directly yield
 212 the globally optimal policy (Lazić et al., 2021). Fortunately, the closed-form solution (5) offers a
 213 simple way to iteratively improve the base policy π_{base} , namely, by iteratively learning and applying
 214 a sequence of value functions, as shown below:
 215

$$216 \quad \pi_t(a_h | s_h) \propto \pi_{t-1}(a_h | s_h) \exp \left(\frac{1}{\beta_{t-1}} V^{\pi_{t-1}}(s_{h+1}) \right) \propto \pi_{\text{base}}(a | s) \exp \left(\sum_{i=0}^{t-1} \frac{1}{\beta_i} V^{\pi_i}(s_{h+1}) \right), \quad (6)$$

216 with $s_{h+1} := [s_h, a_h]$. That is, one can improve the base policy by reweighting it via the exponential
 217 of a *sum* of a sequence of value functions. Further, each value function $V^{\pi_{t-1}}$ is trained using
 218 trajectories sampled from π_{t-1} , as the value estimates depend on that policy’s induced distribution.
 219 In the next section, we will leverage this discussion to develop our proposed algorithm.
 220

221 3 THE PROPOSED ALGORITHM

223 Based on the discussion from the previous section, one can roughly design an algorithm that alternates
 224 between two steps: (i) fitting a value function for the current policy, and (ii) improving the policy via
 225 the TRPO-style update in (5). However, there are a few technical challenges. First, the action space is
 226 extremely large, making exact policy updates computationally infeasible. Second, rewards are often
 227 sparse—typically provided only at the EOS token (Ouyang et al., 2022)—which complicates value
 228 learning due to the long-horizon credit assignment problem.

229 To deal with the first challenge, we avoid the full action space by sampling a small subset of candidates
 230 and performing reweighting only over this sampled subset, retaining the top-scoring candidates in a
 231 beam-search manner. To deal with the second challenge, we train the value function using Monte
 232 Carlo returns obtained from completed trajectories. The proposed algorithm is detailed below.
 233

234 **Value Function Estimation.** Given the dataset $\mathcal{D}_t := \{(\tau_t, r(\tau_t))\}$ at the t -th iteration, where
 235 $\tau_t = (x_t, y_t)$, x_t is sampled from the prompt subset $\mathcal{D}_t^p \subset \mathcal{D}^p$, y_t is the continuation generated by
 236 previous policy $\hat{\pi}_{t-1}$, and $r(\tau_t)$ is the reward score (note, we use $\hat{\pi}_{t-1}$ to denote the estimated version
 237 of the policy π_{t-1} ; for the precise definition please see (8)). The objective of the value training step
 238 is to minimize the discrepancy between the predicted values and the actual return values.

239 We adopt a direct regression approach, where the predicted values are regressed to the observed
 240 returns, following Yang & Klein (2021); Mudgal et al. (2023), which is given by:
 241

$$\hat{V}^{\hat{\pi}_{t-1}} := \arg \min_V \mathbb{E}_{\tau \sim \mathcal{D}_t} \left[\sum_{h=1}^H [V(s_h) - r(\tau)]^2 \right], \quad t = 1, 2, \dots \quad (7)$$

244 where $s_h := [x_t, y_{t,1:h-1}]$ denotes the prefix up to step h . Here, \hat{V} is used as an estimator of the
 245 value function. We will later show that this estimator is theoretically justified.

246 **Data generation and reweighting.** In this step, we aim to update the policy and construct the dataset
 247 $\mathcal{D}_{t+1} := \{\tau_{t+1}, r(\tau_{t+1})\}$. From the previous step, we know that $\hat{V}^{\hat{\pi}_{t-1}}$ is available. Then according
 248 to (6), the log probability of selecting token a_h at state s_h under the estimated policy $\hat{\pi}_t$ is
 249

$$\log \hat{\pi}_t(a_h | s_h) \propto \log \pi_{\text{base}}(a_h | s_h) + \sum_{i=0}^{t-1} \frac{1}{\beta_i} \hat{V}^{\hat{\pi}_i}(s_{h+1}), \quad (8)$$

252 where $\hat{\pi}_0(a_h | s_h) = \pi_{\text{base}}(a_h | s_h)$. Therefore, given a prompt x_{t+1} sampled from $\mathcal{D}_{t+1}^p \subset \mathcal{D}^p$, we
 253 can generate the continuation y_{t+1} using only π_{base} and $\{\hat{V}^{\hat{\pi}_i}\}_{i=0}^{t-1}$. However, updating all actions
 254 $a \in \mathcal{A}$ in the vocabulary at each step is computationally infeasible, especially in LLMs (e.g., the
 255 vocabulary size of GPT4 is 100,256).

257 To effectively generate the sequence y_{t+1} according to (8), we adopt a value-guided beam search
 258 inspired by Zhou et al. (2024). Firstly, initialize K beams given x_{t+1} . For each beam, generate B
 259 candidate successors (token chunks of size L) from π_{base} . Rank the successors using scores computed
 260 as a weighted summation of the outputs from multiple value functions, and select the top- K beams
 261 for the next step. We summarize the proposed algorithm in Algorithm 3 and 4 in Appendix C.

262 We note that the candidate generation step (line 6 in Algorithm 4) often results in identical successors,
 263 which limits the diversity and hinders the exploration. To mitigate this issue, we incorporate a *diversity-*
 264 *first* principle. Specifically, we first cluster identical candidates, and then we prioritize selecting
 265 top-scoring successors across different clusters to maintain diversity (see Figure 7). **Formally, given**
 266 **a candidate set \mathcal{C} , let $g : \mathcal{C} \rightarrow \mathcal{K}$ be a grouping function that maps identical candidates to the same**
 267 **group. For any selected subset $\mathcal{S} \in \mathcal{C}$, we define the diversity measure $\text{Div}(\mathcal{S}) = |\{g(y) : y \in \mathcal{S}\}|$,**
 268 **which is exactly the number of different selected candidates. At the selection stage, we choose the K**
 269 **beams by solving**

$$\mathcal{S}^* = \arg \max_{S \in \mathcal{C}, |\mathcal{S}|=K} [\lambda \cdot \text{Div}(\mathcal{S}) + V(y)], \quad (9)$$

270 where λ is sufficiently large to ensure the diversity. We summarize it in Algorithm 5 in Appendix C.
 271

272 **Value functions compression.** A practical drawback of IRO is that computing the policy $\hat{\pi}_T$ requires
 273 loading all T value functions at inference time, which increases both memory cost and latency. To
 274 mitigate this overhead, we introduce a simple yet effective procedure that compresses multiple value
 275 functions into a single one.

276 Given the rollout datasets from all iterations $\mathcal{D}_{0:T-1}$, we use each trained value functions to annotate
 277 every token in every trajectory. Then we train a single compressed value function to regress toward
 278 these aggregated token-level labels, which can be written as

$$279 \hat{V}^m := \arg \min_V \mathbb{E}_{\tau \sim \mathcal{D}_{0:T-1}} \left[\sum_{h=1}^H \left[\sum_{t=0}^{T-1} \frac{1}{\beta_i} \hat{V}^{\hat{\pi}_i}(s_h) - V(s_h) \right]^2 \right]. \quad (10)$$

282 The compressed value function \hat{V}^m effectively distills the guidance from all iterations into a single
 283 lightweight value function. At inference time, we thus replace all T value functions with just one
 284 compressed value function, significantly reducing both memory cost and latency.
 285

286 4 THEORETICAL ANALYSIS

288 In this section, we present two analyses of the proposed method IRO. First, we conduct a performance
 289 analysis of IRO, demonstrating that it progressively approaches the optimal policy's performance
 290 through multiple iterations. Second, we analyze the sampling and cost efficiency of IRO compared to
 291 the baseline BoN. Through these analyses, we show that IRO achieves strong performance in terms
 292 of both effectiveness and efficiency.
 293

294 4.1 PERFORMANCE ANALYSIS OF IRO

296 To begin with, we introduce the following standard assumptions (Agarwal et al., 2019).

297 **Assumption 1** (Boundedness of Q function class). *Let \mathcal{F} denote a function class to approximate Q
 298 functions. Suppose that $Q^{\pi^t} \in \mathcal{F}$ for all iterations $t \in [T]$. In addition, for any $Q \in \mathcal{F}$, we assume
 299 the values is bounded as $0 \leq Q(s, a) \leq r_{\max}$ for all $s \in \mathcal{S}, a \in \mathcal{A}$.*

300 **Assumption 2** (Concentrability). *Suppose that for all $(s, a) \in (\mathcal{S} \times \mathcal{A})$, the base policy π_{base} can
 301 cover π^* for all $h \in [H]$, i.e., the following holds:*

$$302 \max_{h \in [H]} \frac{d_h^{\pi^*}(s, a)}{d_h^{\pi_{\text{base}}}(s, a)} = C_{\text{ST}} < \infty. \quad (11)$$

305 Next, we proceed to analyze the proposed algorithm. First, recall the discussion after (5), that the
 306 choice of β_t is crucial in controlling the deviation from the base policy. A natural option is to
 307 use a constant $\beta_t = \beta$, under which the algorithm reduces to Natural Policy Gradient (Kakade,
 308 2001), with an $\mathcal{O}(1/t)$ convergence rate established in Xiao (2022) toward the optimal policy for
 309 (1). However, from an empirical perspective (see Section 5), we observe that increasing β_t over time
 310 can lead to more stable improvements in performance. While this adaptive scheme may slow down
 311 convergence to the optimal policy compared to the constant β case, it introduces greater robustness
 312 across iterations. Below, we show that when $\beta_t = \mathcal{O}(\sqrt{t})$, our proposed algorithm still converges to
 313 the global optimum, achieving $\mathcal{O}(T^{-\frac{1}{2}})$ convergence rate to the global optimum.

314 **Theorem 1.** *Suppose Assumption 1 and 2 hold. Consider running the IRO algorithm described in
 315 Algorithm 3 for T iteration, and at each iteration m samples are generated (i.e., $|\mathcal{D}_t^p| = m$). By
 316 choosing $\beta_t = \sqrt{t+1}/\omega$ with $\omega = \sqrt{\frac{2 \log C_{\text{ST}}}{r_{\max}^2 \log T}}$, there exists a $t_0 \in [T]$ with at least probability
 317 $1 - \delta$, such that*

$$318 J(\pi^*) - J(\hat{\pi}_{t_0}) \leq 2\sqrt{r_{\max}^2 H^2 \log T \log C_{\text{ST}}/T} + 2H \sqrt{C_{\text{ST}} \frac{r_{\max}^2}{m} \log \frac{T|\mathcal{F}|}{\delta}}. \quad (12)$$

321 Theorem 1 indicates that the error scales with $1/T$ and $1/m$ polynomially. Specifically, the error
 322 consists of optimization error from the policy update (6) (the first term in (12)), as well as the value
 323 function estimation error (the second term in (12)). This result demonstrates that IRO is a kind of
 324 policy iteration and can converge to the optimal policy.

324 4.2 COST AND SAMPLE EFFICIENCY ANALYSIS OF IRO COMPARED WITH BoN
325

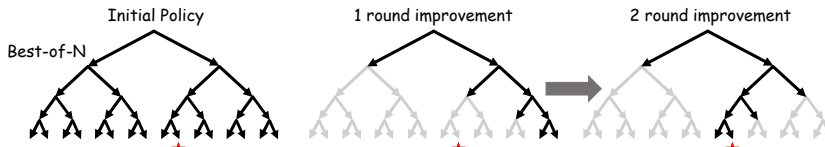
326 Next, we compare the cost and sample efficiency of the proposed method IRO with BoN. Here, we
327 consider the following comparison setting. The BoN generates multiple sequences and then utilizes
328 the reward model to select the best one. For IRO, it trains value functions based on the reward model
329 and then follows the guided generation step to generate desired sequences. We aim to compare the
330 cost of BoN and IRO in order to obtain the desired optimal sequence.

331 Specifically, we define C_{query} as the total number of queries made to the reward model or value
332 functions, and C_{token} as the total token needed to be generated. For example, the BoN method requires
333 $C_{\text{query}}(\text{BoN}) = N$ reward model evaluations, and IRO needs $C_{\text{query}}(\text{IRO}) = BKHI$, where I is the
334 number of value functions used, H is the horizon, K is the beam width, and B is the number of
335 successors per step. The proof can be found in the Appendix B.3.

336 **Proposition 1.** *Consider a finite horizon H setting. Let IRO perform guided generation using I
337 value functions, where the weighted combination of I value functions approximate the gold value
338 function, i.e., $\sum_{i=0}^{I-1} \frac{1}{\beta_i} V_i \approx V^*$. Let decoding proceed in chunks of length L , with beam width K ,
339 and B successors per step, as illustrated in Alg. 4. To achieve an equal probability of sampling the
340 optimal sequence, the relative query cost and token number of the two algorithms satisfy:*

$$341 \quad \frac{C_{\text{query}}(\text{BoN})}{C_{\text{query}}(\text{IRO})} = \frac{L}{HI} (BK)^{H/L-1}, \quad \frac{C_{\text{token}}(\text{BoN})}{C_{\text{token}}(\text{IRO})} = (BK)^{H/L-1}. \quad (13)$$

344 As shown in the above proposition, under ideal situations, where I value functions approximate V^* ,
345 IRO achieves higher cost-efficiency than BoN. While the query cost of IRO increases with the number
346 of value functions I , the token cost ratio remains unaffected. This advantage becomes especially
347 significant as the horizon H increases while the chunk length L remains fixed, as illustrated in Fig.
348 2. Besides this, we provide a detailed comparison of computational cost between IRO and other
349 inference-time methods in Appendix E.



351
352
353
354
355
356 Figure 2: Illustration that IRO is more sample-efficient than BoN. With action space $|\mathcal{A}| = 2$ and
357 horizon $H = 4$, BoN traverses all 30 nodes to find the optimal generation. IRO trains value functions
358 to guide policy to search, prunes the search space, and reaches the optimal solution with only 8 nodes
359 via continual value function updates.

360 **Remark 4.1.** *In practice, generation quality may fall short of the theoretical guarantee for the
361 following reasons: (1) The IRO is only ran for a few iterations, generating few value functions that
362 may not be able to accurately approximate V^* , leading to suboptimal candidate selection; and
363 (2) The reweighting is performed over a sampled subset of the action space rather than the full
364 vocabulary, which introduces additional approximation error during decoding.*

365 5 EXPERIMENT
366

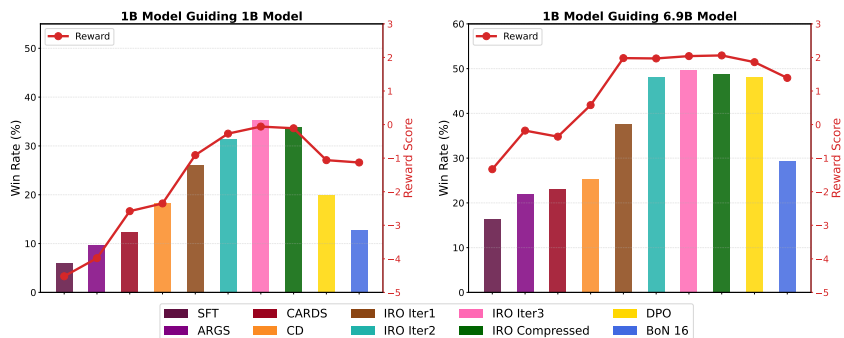
367 In this section, we provide numerical evaluations of the proposed method IRO. Our experiments
368 demonstrate its effectiveness and flexibility on the TL;DR summarization dataset (Stiennon et al.,
369 2020) and the UltraFeedback dataset (Cui et al., 2023). Specifically, IRO shows: (1) strong weak-
370 to-strong generalization, such as when using 1B value functions to guide a 1B policy model, and
371 using 7B value functions to guide a 70B model. (2) IRO scales effectively with the search compute
372 budget (e.g., $U = KB$ in the guided generation step). In addition to tasks with continuous rewards,
373 we also discuss the IRO’s generalization to verifiable reward setting in Appendix H.4.

374 375 5.1 ALIGNING LLM WITH TL;DR DATASET
376

377 In this experiment, we consider two settings: (1) using 1B value functions to guide a 1B policy, and
378 (2) using 1B value functions to guide a 6.9B policy. We defer more details to Appendix H.1.

378 **Model and Datasets.** We use the SFT model based on EleutherAI/pythia family with size 1B
 379 and 6.9B, fine-tuned on TL;DR text-summarization dataset following the methodology outlined in
 380 Huang et al. (2024b). We use a Pythia-1b based reward model to serve as the reward $r(\cdot)$ needed
 381 to run the IRO algorithm.

382 **Baselines and Evaluation** Our baselines include BoN, three token-level inference-time methods
 383 ARGs (Khanov et al., 2024), CARDS (Li et al., 2024), controlled decoding (CD; Mudgal et al.
 384 (2023)), and train-based method DPO. Evaluation is based on the win rate of the model-generated
 385 summary against the reference summary, evaluated by GPT-4o-mini (see Appendix G for details).
 386



387 Figure 3: Gold reward score evaluated by a 6.9B reward model (line) and win rates (bar) evaluated by
 388 GPT-4o-mini across multiple iterations on 300 samples from the test dataset. The decoding proceeds
 389 with $K = 4$ and $B = 4$. For the IRO, we train the algorithm in 3 iterations. During testing, in order
 400 to show the benefit of running multiple training iterations, we first evaluate the policy with 1 value
 401 function (we call iter 1), and then more value functions (iter 2 and iter 3). We adopt $\beta_i = 1$ for all
 402 iterations.
 403

404 **Results.** As shown in Fig. 3, our method outperforms both the inference-time baseline, including
 405 BoN, ARGs, and CARDS, as well as the training-time method DPO. It achieves consistent gains in
 406 both reward scores evaluated by a gold reward model and win rate across iterations, which align with
 407 our goal of iterative policy improvement (6). For example, with 1B value functions’ guidance, IRO
 408 improves the win rate over DPO by 14%. In the weak-to-strong setting (1B value functions guiding
 409 the 6.9B policy), it surpasses the DPO by the third iteration on win rate by 2%, demonstrating strong
 410 generalization even with a smaller value model. Notably, using only one compressed value function
 411 results in only a 1.67% drop in win rate for the 1B policy and 0.9% for the 6.9B policy, while still
 412 outperforming IRO Iter2. This shows that the compressed value function retains most information
 413 from previous value functions, greatly reducing computational cost.
 414

415 5.2 ALIGNING LLM WITH ULTRAFEEDBACK DATASET

416 Further, to evaluate the effectiveness of IRO at scale, we conduct a scaled-up experiment. Specifically,
 417 7B value models are used to guide the generation of 8B and 70B models. We defer more details to
 418 Appendix H.2.
 419

420 **Model and Datasets.** We use Llama-3-8B-Instruct and Llama-3-70B-Instruct as
 421 base policies. The reward model is initialized from Mistral-7B-v0.1 and trained with UltraFeedback
 422 dataset (Cui et al., 2023).
 423

424 **Baseline.** We consider the following baselines: (1) BoN with explicit rewards (BoN-E) and implicit
 425 rewards (BoN-I), where the implicit reward is calculated as log-probability difference between a base
 426 model and a fine-tuned model (Rafailov et al., 2024a); (2) search-based methods Weak-to-Strong
 427 Search (Zhou et al., 2024); (3) token-level based method ARGs (Khanov et al., 2024) and controlled
 428 decoding (CD; Mudgal et al. (2023)).
 429

430 **Evaluation.** We evaluate the performance on a standard single-turn instruction-following benchmark,
 431 AlpacaEval 2.0 (Li et al., 2023), which consists of 805 prompts from various open-source datasets.
 432 Our evaluation reports the length-controlled (LC) win rate (Dubois et al., 2024), which is a metric
 433 specifically designed to mitigate biases arising from model verbosity.
 434

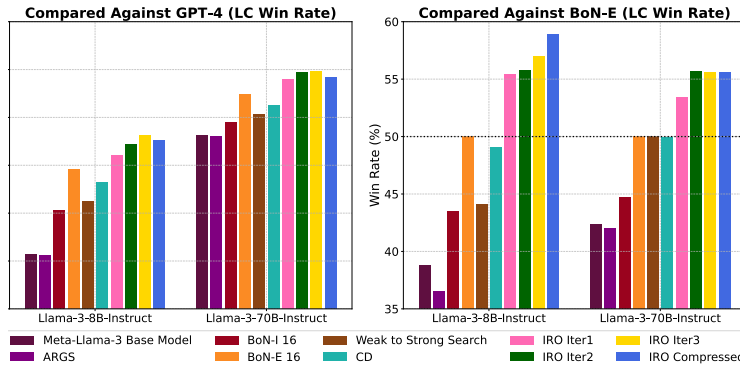


Figure 4: AlpacaEval 2 length-controlled win rate compared against GPT-4 (left) and BoN-E (right) on both 7B and 70B base models, evaluated by GPT-4. We use $\beta_1 = 1, \beta_2 = 2, \beta_3 = 2.5$.

Results. As shown in Fig. 4, IRO demonstrates consistent and substantial improvements over the baseline compared against the response generated by GPT-4. Notably, BoN-E is a strong baseline since it significantly outperforms other inference-time algorithms (this result is consistent with findings reported in prior work (Xu et al., 2024b; Liu et al., 2024)). For the IRO, its performance continues to improve as we add value functions to improve the quality of the guidance. This confirms our intuition that rather than requiring additional computational resources to fine-tune the model during training, significant improvements can be achieved successively through value-guided exploration at inference time. Here, we adopt an increasing parameter β_t as iterations proceed. This more conservative strategy becomes necessary to ensure stability and prevent excessive deviation from the previous policy. In addition, the compressed value function retains nearly all the benefits of multi-iteration IRO while requiring only a single model at inference time: its win rates drop by only 0.2–1.0% compared with Iter3, while slightly exceeding those of Iter2. This makes IRO more practical, which preserves performance while significantly reducing inference overhead.

5.3 EFFICIENCY ANALYSIS

In this section, we empirically evaluate the inference-time efficiency of IRO in terms of decoding latency and peak memory usage compared with BoN and vanilla generation. As shown in Fig. 5, although increasing the number of iterations consistently improves alignment performance, it also leads to higher latency and memory usage. Importantly, our proposed compressing multiple value functions effectively mitigates this overhead.

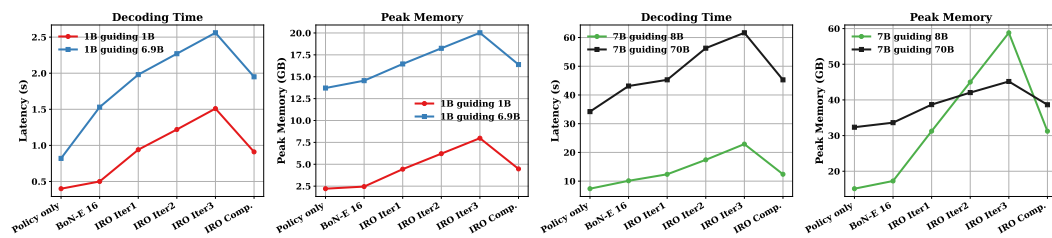


Figure 5: Inference-time latency and peak memory usage. All experiments are conducted over 30 samples on one H100 GPU, except for the 7B guiding 70B configuration, which is measured on 4 H100 GPUs.

5.4 TEST-TIME SCALING WITH VALUE FUNCTION

In this section, we explore how the generation quality of IRO, measured by win rate against references and the reward score evaluated by a gold reward model, scales with the search compute budget $U := KB$ across different iterations. Here, both BoN and IRO use the same total number of UH tokens for fair comparison. As shown in Fig. 6 and Fig. 11, increasing the search compute budget

U leads to improvements in both reward scores, which serves as a proxy for generation quality as judged by a gold reward model, and win rate evaluated by GPT-4, indicating the effectiveness of using value functions to guide generation. While the BoN baseline also benefits from a larger search compute budget *U*, its performance saturates early and remains notably below that of IRO. Notably, the value function from the first iteration underperforms in higher budgets (larger *U*), likely due to the limited training data, subsequent iterations effectively correct this and achieve better performance. This iterative improving mechanism can be further illustrated in Fig. 2, where subsequent value functions correct suboptimal paths introduced by earlier guidance.

This empirical observation aligns with our theoretical analysis in Sec. 4: as the number of iterations increases, IRO exhibits convergence behavior, with improved generation quality guided by sequences of value functions. Moreover, the observed trend between win rate and search compute budget *U* confirms that IRO achieves higher sample efficiency than BoN under comparable compute budgets.

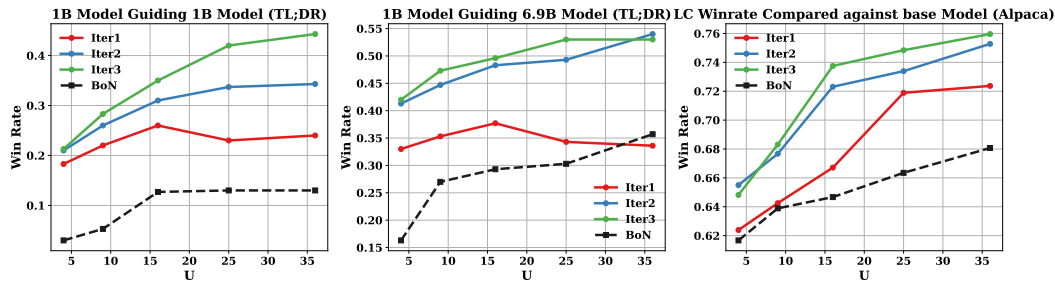


Figure 6: Win rate judged by GPT-4o-mini on the TL; DR task and GPT-4 on the Alpaca subset, showing improvements with increased search compute budget *U* under three iterations and BoN algorithm. During the search, we set the parameters $K = B = \sqrt{U}$. The first two plots compare against reference summaries, while the third compares against standard generation.

5.5 ABLATION STUDY

Due to the page limit, we defer more ablation studies and details to the Appendix H.5.

Explore different sampling strategies for IRO. We compare four sampling approaches: beam search (Zhou et al., 2024) with and without the *diversity-first* principle, and stochastic sampling methods with different temperatures. As shown in Fig. 12, incorporating the *diversity-first* principle into beam search significantly improves performance, while stochastic sampling methods are highly sensitive to the temperature parameter T_{temp} .

Robustness of IRO under imperfect reward model. To assess robustness, we evaluate IRO using reward models of varying quality on the summarization task (see Table 8 and Table 9) and Instruct-following task (see Table 14). As expected, stronger reward models lead to larger gains in the first iteration. More importantly, even weaker models still enable consistent improvement under the iterative procedure. **Thus, while IRO is robust to imperfect reward supervision, the ultimate performance is still bounded by the quality of the reward model, which defines the upper limit of alignment quality.**

6 CONCLUSION

In this paper, we introduced Iterative Reweighting-then-Optimize (IRO), a Reinforcement Learning framework-style alignment of the frozen model at inference time. By learning a sequence of value functions, IRO enables successive policy improvement. We prove that IRO theoretically converges to the optimal policy under certain standard assumptions, and requires exponentially fewer tokens and external function queries than BoN when achieving comparable performance as BoN. **In addition, by compressing multiple value functions into a single one, IRO substantially reduces inference-time memory usage and latency while maintaining competitive performance.** Empirically, we demonstrate the strong effectiveness of IRO through extensive experiments and ablation studies.

540 REFERENCES
541

542 Josh Achiam, Steven Adler, Sandhini Agarwal, Lama Ahmad, Ilge Akkaya, Florencia Leoni Aleman,
543 Diogo Almeida, Janko Altenschmidt, Sam Altman, Shyamal Anadkat, et al. Gpt-4 technical report.
544 *arXiv preprint arXiv:2303.08774*, 2023.

545 Alekh Agarwal, Nan Jiang, Sham M Kakade, and Wen Sun. Reinforcement learning: Theory and
546 algorithms. *CS Dept., UW Seattle, Seattle, WA, USA, Tech. Rep*, 32, 2019.

547 Arash Ahmadian, Chris Cremer, Matthias Gallé, Marzieh Fadaee, Julia Kreutzer, Olivier Pietquin,
548 Ahmet Üstün, and Sara Hooker. Back to basics: Revisiting reinforce style optimization for learning
549 from human feedback in llms. *arXiv preprint arXiv:2402.14740*, 2024.

550 Mohammad Gheshlaghi Azar, Mark Rowland, Bilal Piot, Daniel Guo, Daniele Calandriello, Michal
551 Valko, and Rémi Munos. A general theoretical paradigm to understand learning from human
552 preferences. *arXiv preprint arXiv:2310.12036*, 2023.

553 Jinze Bai, Shuai Bai, Yunfei Chu, Zeyu Cui, Kai Dang, Xiaodong Deng, Yang Fan, Wenbin Ge,
554 Yu Han, Fei Huang, et al. Qwen technical report. *arXiv preprint arXiv:2309.16609*, 2023.

555 Yuntao Bai, Andy Jones, Kamal Ndousse, Amanda Askell, Anna Chen, Nova DasSarma, Dawn Drain,
556 Stanislav Fort, Deep Ganguli, Tom Henighan, et al. Training a helpful and harmless assistant with
557 reinforcement learning from human feedback. *arXiv preprint arXiv:2204.05862*, 2022.

558 Souradip Chakraborty, Soumya Suvra Ghosal, Ming Yin, Dinesh Manocha, Mengdi Wang, Amit
559 Singh Bedi, and Furong Huang. Transfer q star: Principled decoding for llm alignment. *arXiv
560 preprint arXiv:2405.20495*, 2024.

561 Jonathan D Chang, Wenhao Zhan, Owen Oertell, Kianté Brantley, Dipendra Misra, Jason D Lee, and
562 Wen Sun. Dataset reset policy optimization for rlhf. *arXiv preprint arXiv:2404.08495*, 2024.

563 Jie Cheng, Ruixi Qiao, Lijun Li, Chao Guo, Junle Wang, Gang Xiong, Yisheng Lv, and Fei-Yue Wang.
564 Stop summation: Min-form credit assignment is all process reward model needs for reasoning.
565 *arXiv preprint arXiv:2504.15275*, 2025.

566 Ganqu Cui, Lifan Yuan, Ning Ding, Guanming Yao, Wei Zhu, Yuan Ni, Guotong Xie, Zhiyuan Liu,
567 and Maosong Sun. Ultrafeedback: Boosting language models with high-quality feedback. 2023.

568 Hanze Dong, Wei Xiong, Bo Pang, Haoxiang Wang, Han Zhao, Yingbo Zhou, Nan Jiang, Doyen
569 Sahoo, Caiming Xiong, and Tong Zhang. Rlhf workflow: From reward modeling to online rlhf,
2024.

570 Yann Dubois, Chen Xuechen Li, Rohan Taori, Tianyi Zhang, Ishaan Gulrajani, Jimmy Ba, Carlos
571 Guestrin, Percy S Liang, and Tatsunori B Hashimoto. Alpacafarm: A simulation framework for
572 methods that learn from human feedback. *Advances in Neural Information Processing Systems*,
573 36:30039–30069, 2023.

574 Yann Dubois, Balázs Galambosi, Percy Liang, and Tatsunori B Hashimoto. Length-controlled
575 alpacaeval: A simple way to debias automatic evaluators. *arXiv preprint arXiv:2404.04475*, 2024.

576 Leo Gao, John Schulman, and Jacob Hilton. Scaling laws for reward model overoptimization. In
577 *International Conference on Machine Learning*, pp. 10835–10866. PMLR, 2023.

578 Daya Guo, Dejian Yang, Huawei Zhang, Junxiao Song, Ruoyu Zhang, Runxin Xu, Qihao Zhu,
579 Shirong Ma, Peiyi Wang, Xiao Bi, et al. Deepseek-r1: Incentivizing reasoning capability in llms
580 via reinforcement learning. *arXiv preprint arXiv:2501.12948*, 2025.

581 Seungwook Han, Idan Shenfeld, Akash Srivastava, Yoon Kim, and Pulkit Agrawal. Value augmented
582 sampling for language model alignment and personalization. *arXiv preprint arXiv:2405.06639*,
583 2024.

584 Joey Hejna and Dorsa Sadigh. Inverse preference learning: Preference-based rl without a reward
585 function. *Advances in Neural Information Processing Systems*, 36, 2024.

594 James Y Huang, Sailik Sengupta, Daniele Bonadiman, Yi-an Lai, Arshit Gupta, Nikolaos Pappas,
 595 Saab Mansour, Katrin Kirchhoff, and Dan Roth. Deal: Decoding-time alignment for large language
 596 models. *arXiv preprint arXiv:2402.06147*, 2024a.

597

598 Shengyi Huang, Michael Noukhovitch, Arian Hosseini, Kashif Rasul, Weixun Wang, and Lewis
 599 Tunstall. The n+ implementation details of rlhf with ppo: A case study on tl; dr summarization.
 600 *arXiv preprint arXiv:2403.17031*, 2024b.

601 Dongfu Jiang, Xiang Ren, and Bill Yuchen Lin. Llm-blender: Ensembling large language models
 602 with pairwise ranking and generative fusion. *arXiv preprint arXiv:2306.02561*, 2023.

603

604 Sham M Kakade. A natural policy gradient. *Advances in neural information processing systems*, 14,
 605 2001.

606 Maxim Khanov, Jirayu Burapachep, and Yixuan Li. Args: Alignment as reward-guided search.
 607 *arXiv preprint arXiv:2402.01694*, 2024.

608

609 Lingkai Kong, Haorui Wang, Wenhao Mu, Yuanqi Du, Yuchen Zhuang, Yifei Zhou, Yue Song,
 610 Rongzhi Zhang, Kai Wang, and Chao Zhang. Aligning large language models with representation
 611 editing: A control perspective. *arXiv preprint arXiv:2406.05954*, 2024.

612 Nevena Lazić, Botao Hao, Yasin Abbasi-Yadkori, Dale Schuurmans, and Csaba Szepesvári. Opti-
 613 mization issues in kl-constrained approximate policy iteration. *arXiv preprint arXiv:2102.06234*,
 614 2021.

615 Bolian Li, Yifan Wang, Anamika Lochab, Ananth Grama, and Ruqi Zhang. Cascade reward sampling
 616 for efficient decoding-time alignment. *arXiv preprint arXiv:2406.16306*, 2024.

617

618 Xuechen Li, Tianyi Zhang, Yann Dubois, Rohan Taori, Ishaan Gulrajani, Carlos Guestrin, Percy
 619 Liang, and Tatsunori B Hashimoto. Alpacaeval: An automatic evaluator of instruction-following
 620 models, 2023.

621 Hunter Lightman, Vineet Kosaraju, Yuri Burda, Harrison Edwards, Bowen Baker, Teddy Lee, Jan
 622 Leike, John Schulman, Ilya Sutskever, and Karl Cobbe. Let's verify step by step. In *The Twelfth
 623 International Conference on Learning Representations*, 2023.

624

625 Zhixuan Liu, Zhanhui Zhou, Yuanfu Wang, Chao Yang, and Yu Qiao. Inference-time language model
 626 alignment via integrated value guidance. *arXiv preprint arXiv:2409.17819*, 2024.

627

628 Sidharth Mudgal, Jong Lee, Harish Ganapathy, YaGuang Li, Tao Wang, Yanping Huang, Zhifeng
 629 Chen, Heng-Tze Cheng, Michael Collins, Trevor Strohman, et al. Controlled decoding from
 630 language models. *arXiv preprint arXiv:2310.17022*, 2023.

631

632 Reiichiro Nakano, Jacob Hilton, Suchir Balaji, Jeff Wu, Long Ouyang, Christina Kim, Christopher
 633 Hesse, Shantanu Jain, Vineet Kosaraju, William Saunders, et al. Webgpt: Browser-assisted
 634 question-answering with human feedback. *arXiv preprint arXiv:2112.09332*, 2021.

635

636 Long Ouyang, Jeffrey Wu, Xu Jiang, Diogo Almeida, Carroll Wainwright, Pamela Mishkin, Chong
 637 Zhang, Sandhini Agarwal, Katarina Slama, Alex Ray, et al. Training language models to follow
 638 instructions with human feedback. *Advances in Neural Information Processing Systems*, 35:
 27730–27744, 2022.

639

640 Jiahao Qiu, Yifu Lu, Yifan Zeng, Jiacheng Guo, Jiayi Geng, Huazheng Wang, Kaixuan Huang, Yue
 641 Wu, and Mengdi Wang. Treebon: Enhancing inference-time alignment with speculative tree-search
 642 and best-of-n sampling. *arXiv preprint arXiv:2410.16033*, 2024.

643

644 Rafael Rafailov, Joey Hejna, Ryan Park, and Chelsea Finn. From r to q^* : Your language model is
 645 secretly a q-function. *arXiv preprint arXiv:2404.12358*, 2024a.

646

647 Rafael Rafailov, Archit Sharma, Eric Mitchell, Christopher D Manning, Stefano Ermon, and Chelsea
 648 Finn. Direct preference optimization: Your language model is secretly a reward model. *Advances
 649 in Neural Information Processing Systems*, 36, 2024b.

650

John Schulman. Trust region policy optimization. *arXiv preprint arXiv:1502.05477*, 2015.

648 John Schulman, Philipp Moritz, Sergey Levine, Michael Jordan, and Pieter Abbeel. High-dimensional
 649 continuous control using generalized advantage estimation. *arXiv preprint arXiv:1506.02438*,
 650 2015.

651

652 John Schulman, Filip Wolski, Prafulla Dhariwal, Alec Radford, and Oleg Klimov. Proximal policy
 653 optimization algorithms. *arXiv preprint arXiv:1707.06347*, 2017.

654 Lior Shani, Yonathan Efroni, and Shie Mannor. Adaptive trust region policy optimization: Global
 655 convergence and faster rates for regularized mdps. In *Proceedings of the AAAI Conference on*
 656 *Artificial Intelligence*, volume 34, pp. 5668–5675, 2020.

657

658 Zhihong Shao, Peiyi Wang, Qihao Zhu, Runxin Xu, Junxiao Song, Xiao Bi, Haowei Zhang,
 659 Mingchuan Zhang, YK Li, Y Wu, et al. Deepseekmath: Pushing the limits of mathematical
 660 reasoning in open language models. *arXiv preprint arXiv:2402.03300*, 2024.

661 Charlie Snell, Jaehoon Lee, Kelvin Xu, and Aviral Kumar. Scaling llm test-time compute optimally
 662 can be more effective than scaling model parameters. *arXiv preprint arXiv:2408.03314*, 2024.

663

664 Yuda Song, Yifei Zhou, Ayush Sekhari, J Andrew Bagnell, Akshay Krishnamurthy, and Wen Sun.
 665 Hybrid rl: Using both offline and online data can make rl efficient. *arXiv preprint arXiv:2210.06718*,
 666 2022.

667 Nisan Stiennon, Long Ouyang, Jeffrey Wu, Daniel Ziegler, Ryan Lowe, Chelsea Voss, Alec Radford,
 668 Dario Amodei, and Paul F Christiano. Learning to summarize with human feedback. *Advances in*
 669 *Neural Information Processing Systems*, 33:3008–3021, 2020.

670

671 Kaiwen Wang, Jin Peng Zhou, Jonathan Chang, Zhaolin Gao, Nathan Kallus, Kianté Brantley,
 672 and Wen Sun. Value-guided search for efficient chain-of-thought reasoning. *arXiv preprint*
 673 *arXiv:2505.17373*, 2025.

674 Jason Wei, Xuezhi Wang, Dale Schuurmans, Maarten Bosma, Fei Xia, Ed Chi, Quoc V Le, Denny
 675 Zhou, et al. Chain-of-thought prompting elicits reasoning in large language models. *Advances in*
 676 *neural information processing systems*, 35:24824–24837, 2022.

677

678 Lin Xiao. On the convergence rates of policy gradient methods. *Journal of Machine Learning*
 679 *Research*, 23(282):1–36, 2022.

680 Shusheng Xu, Wei Fu, Jiaxuan Gao, Wenjie Ye, Weilin Liu, Zhiyu Mei, Guangju Wang, Chao Yu,
 681 and Yi Wu. Is dpo superior to ppo for llm alignment? a comprehensive study. *arXiv preprint*
 682 *arXiv:2404.10719*, 2024a.

683

684 Yuancheng Xu, Udari Madhushani Sehwag, Alec Koppel, Sicheng Zhu, Bang An, Furong Huang,
 685 and Sumitra Ganesh. Genarm: Reward guided generation with autoregressive reward model for
 686 test-time alignment. *arXiv preprint arXiv:2410.08193*, 2024b.

687

688 Kevin Yang and Dan Klein. Fudge: Controlled text generation with future discriminators. *arXiv*
 689 *preprint arXiv:2104.05218*, 2021.

690

691 Xinnan Zhang, Siliang Zeng, Jiaxiang Li, Kaixiang Lin, and Mingyi Hong. Llm alignment through
 692 successive policy re-weighting (spr). In *NeurIPS 2024 Workshop on Fine-Tuning in Modern*
 693 *Machine Learning: Principles and Scalability*, 2024.

694

695 Jin Peng Zhou, Kaiwen Wang, Jonathan D Chang, Zhaolin Gao, Nathan Kallus, Kilian Q Weinberger,
 696 Kianté Brantley, and Wen Sun. q: Provably optimal distributional rl for llm post-training. *CoRR*,
 697 2025.

698

699 Zhanhui Zhou, Zhixuan Liu, Jie Liu, Zhichen Dong, Chao Yang, and Yu Qiao. Weak-to-strong
 700 search: Align large language models via searching over small language models. *arXiv preprint*
 701 *arXiv:2405.19262*, 2024.

702 Banghua Zhu, Evan Frick, Tianhao Wu, Hanlin Zhu, and Jiantao Jiao. Starling-7b: Improving llm
 703 helpfulness & harmlessness with rlaif. 2023, 2023.

702 A RELATED WORK
703704 A.1 REINFORCEMENT LEARNING WITH HUMAN FEEDBACK
705

706 Reinforcement learning from human feedback (RLHF) (Stiennon et al., 2020; Ouyang et al., 2022) is
707 a widely adopted technique for fine-tuning AI systems to align with human preferences and values.
708 Current RLHF approaches typically involve training a reward model using human preference feedback
709 and then fine-tuning the language model via proximal policy optimization (PPO) (Schulman et al.,
710 2017). In addition to PPO, other reinforcement learning solvers such as RLOO (Ahmadian et al.,
711 2024) and GRPO (Shao et al., 2024) have also demonstrated effectiveness in advanced foundation
712 language models. However, optimizing these algorithms for peak performance requires substantial
713 effort and resources, which are often beyond the reach of the open-source community.

714
715 A.2 TRAINING-TIME ALIGNMENT
716

717 In an effort to reduce computational overhead in reinforcement learning, alternative alignment strate-
718 gies such as Direct Preference Optimization (DPO) (Rafailov et al., 2024b) and Inverse Preference
719 Learning (IPL) (Hejna & Sadigh, 2024) remove the need for explicit reward modeling by extracting
720 policies directly from preference data. While this substantially lowers training complexity, these algo-
721 rithms can be unstable during training (Azar et al., 2023; Xu et al., 2024a), and once the preference
722 dataset is fixed, they offer limited opportunities for further policy improvement.

723
724 A.3 INFERENCE-TIME ALIGNMENT
725

726 Although training-time alignment methods are effective, they demand substantial computational and
727 engineering resources. To mitigate these costs, inference-time alignment approaches typically freeze
728 pre-trained models and adjust their outputs during a decoding or test phase, which is handled by
729 smaller, specialized models (Khanov et al., 2024; Mudgal et al., 2023).

730 The conceptual framework for aligning language models at inference time is rooted in the use of
731 value function (Mudgal et al., 2023) or outcome reward function (Khanov et al., 2024). Based on the
732 type of model used to guide the frozen LLM, we categorize related work into two main approaches:
733 (1) outcome reward guidance, and (2) value function and PRM-based guidance.

734
735 A.3.1 OUTCOME REWARD GUIDANCE
736

737 Based on ORM, a widely used approach, Best-of- N (BoN) (Nakano et al., 2021; Stiennon et al., 2020),
738 samples N candidate completions and selects the one with the highest ORM score. While effective,
739 BoN operates at the *response level* and requires a large N (e.g., 1,000–60,000 (Gao et al., 2023;
740 Dubois et al., 2023)) to match training-time performance, resulting in high inference cost and latency.
741 To address this, several methods (Khanov et al., 2024; Liu et al., 2024; Xu et al., 2024b; Li et al.,
742 2024) incorporate *token-level* guidance using only the ORM. ARGs (Khanov et al., 2024) constructs
743 a token-level score function by applying the ORM to partial generations. However, since the ORM is
744 trained only on full outputs, its predictions on incomplete sequences are often unreliable, leading to
745 suboptimal guidance. Furthermore, these methods require the same vocabulary as the frozen LLM,
746 which is often inaccessible in practice, especially for proprietary or closed-source models (Achiam
747 et al., 2023; Bai et al., 2022). Other approaches compute accurate token-level rewards by generating
748 full continuations for each token candidate and scoring them with the ORM (Chakraborty et al., 2024;
749 Huang et al., 2024a). This strategy improves fidelity but introduces prohibitive inference overhead,
750 scaling poorly with sequence length and vocabulary size.

751 An alternative, but less relevant, line of work leverages *implicit* rewards, such as the log-probability
752 difference between a base model and a fine-tuned model (Rafailov et al., 2024a; Qiu et al., 2024;
753 Zhou et al., 2024; Liu et al., 2024). However, they often misalign with human preferences and can
754 even degrade performance relative to explicit reward models (Liu et al., 2024). This discrepancy
755 arises because log-probability gaps reflect likelihood differences rather than true utility or preference,
and thus may reward verbosity, repetition, or high-likelihood but unhelpful completions.

756 A.3.2 VALUE FUNCTION AND PRM-BASED GUIDANCE
757

758 Another closely related line of work for inference-time alignment is to train an external value
759 function, sometimes also called a process reward model (PRM) to guide generation (Mudgal et al.,
760 2023; Han et al., 2024; Kong et al., 2024; Zhou et al., 2025; Wang et al., 2025). A value function
761 estimates the expected future contribution from a given partial response, enabling more informed
762 token selection during inference. However, applying these methods in practice faces two major
763 challenges. First, training a high-quality value function or PRM—especially one that operates at
764 the step level—typically requires large-scale and fine-grained human-labeled data. For instance,
765 OpenAI’s PRM800K dataset (Lightman et al., 2023) was constructed through extensive manual
766 annotation of intermediate reasoning steps, incurring substantial labor and financial costs. This kind
767 of supervision is only feasible in tasks with well-defined reasoning paths, such as math or code
768 generation, and is difficult to generalize to open-ended instruction-following or dialog tasks where
769 step quality is ambiguous. Second, even when a value function or PRM is available, most existing
770 approaches apply it *only once* during decoding. That is, these models are used to resample or filter
771 outputs in a single pass, rather than continuously refining the generation process. Because these
772 models are often imperfect—due to limited training data, model capacity, or domain shift—this
773 single-round guidance can result in suboptimal outputs, especially in challenging or long-horizon
774 tasks.

775 B PROOF
776777 B.1 PROOF OF (5)
778

779 *Proof.* In this section, we provide the full derivation of the KL-constrained optimization formulation
780 used in our method. At each policy iteration step, given the current policy π_{old} , we aim to maximize
781 the performance gap $\max_{\pi} \eta^{\pi}(\pi) := J(\pi) - J(\pi_{\text{old}})$. Following the TRPO (Schulman, 2015)
782 formulation, we consider sampling the data from the visitation measure $d_h^{\pi_{\text{old}}}$ induced by the current
783 policy. This leads to the following KL-constrained optimization problem:

$$784 \max_{\pi} \tilde{\eta}^{\pi_{\text{old}}}(\pi) \quad (14a)$$

$$785 \text{s.t.} \quad \sum_{h=1}^H \mathbb{E}_{s_h \sim d_h^{\pi_{\text{old}}}} [D_{\text{KL}}(\pi(\cdot|s_h) || \pi_{\text{old}}(\cdot|s_h))] \leq \epsilon, \quad (14b)$$

$$786 \sum_{a \in \mathcal{A}} \pi(a|s) = 1, \forall s \in \mathcal{S}_h, \quad (14c)$$

$$787 \pi(a|s_h) \geq 0, \forall s \in \mathcal{S}_h, a \in \mathcal{A} \quad \text{for all } h \in [H], \quad (14d)$$

788 where $\tilde{\eta}^{\pi_{\text{old}}}(\pi) = \sum_{h=1}^H \mathbb{E}_{s_h \sim d_h^{\pi_{\text{old}}}, a_h \sim \pi(\cdot|s_h)} [A^{\pi_{\text{old}}}(s_h, a_h)]$, s_h is the visitation measure for the
789 state at the h th timestep, $d_h^{\pi_{\text{old}}} = \sum_{a \in \mathcal{A}} \mathbb{E}_{s_1 \sim \mu} [\mathcal{P}^{\pi}(s_h = s, a_h = a|s_1)]$.

790 To derive the solution, we first write down the *partial* Lagrangian function, which only considers
791 the constraints (14b)-(14c). After solving the partial Lagrangian function, we will show that the
792 constraint (14d) is satisfied.

793 Let β and $\zeta := \{\zeta_{s,h} | s \in \mathcal{S}_h\}$ denote the dual variables of the constraints (14b) and (14c), respectively.
794 Then the partial Lagrangian function can be expressed as below:

$$795 \mathcal{L}(\pi, \beta, \zeta) := \sum_{h=1}^H \mathbb{E}_{s_h \sim d_h^{\pi_{\text{base}}}, a \sim \pi(\cdot|s_h)} [A^{\pi_{\text{base}}}(s_h, a_h)] + \beta \left(\epsilon - \sum_{h=1}^H \mathbb{E}_{s_h \sim d_h^{\pi_{\text{base}}}} [D_{\text{KL}}(\pi(\cdot|s_h) || \pi_{\text{base}}(\cdot|s_h))] \right)$$

$$796 + \sum_{h=1}^H \sum_{s \in \mathcal{S}_h} \zeta_{s,h} \left(1 - \sum_{a \in \mathcal{A}} \pi(a|s_h) \right).$$

797 Through taking partial derivative of $\mathcal{L}(\pi, \beta, \zeta)$ w.r.t. $\pi(a_h|s_h)$, we can obtain the following equation:

$$798 \frac{\partial \mathcal{L}(\pi, \beta, \zeta)}{\partial \pi(a_h|s_h)} = d_h^{\pi_{\text{base}}}(s_h) A^{\pi_{\text{base}}}(s_h, a_h) - \beta d_h^{\pi_{\text{base}}}(s_h) \left(-\log \pi_{\text{base}}(a_h|s_h) + \log \pi(a_h|s_h) + 1 \right) - \zeta_{s,h}.$$

810 Through setting the partial derivative $\frac{\partial \mathcal{L}(\pi, \beta, \zeta)}{\partial \pi(a_h|s_h)}$ to 0, we obtain
 811

$$812 \quad 813 \quad d^{\pi_{\text{base}}}(s_h) A^{\pi_{\text{base}}}(s_h, a_h) - \beta d^{\pi_{\text{base}}}(s_h) \left(-\log \pi_{\text{base}}(a_h|s_h) + \log \pi(a_h|s_h) + 1 \right) - \zeta_{s,h} = 0. \\ 814$$

815 Then we obtain the closed-form expression of the optimal policy π^* as below:
 816

$$817 \quad \log \pi^*(a_h|s_h) = \frac{A^{\pi_{\text{base}}}(s_h, a_h)}{\beta} + \log \pi_{\text{base}}(a_h|s_h) - 1 - \frac{\zeta_{s,h}}{\beta d^{\pi_{\text{base}}}(s_h)}, \quad (15a)$$

$$819 \quad 820 \quad \pi^*(a_h|s_h) = \pi_{\text{base}}(a_h|s_h) \exp \left(\frac{A^{\pi_{\text{base}}}(s_h, a_h)}{\beta} \right) \exp \left(-1 - \frac{\zeta_{s,h}}{\beta d^{\pi_{\text{base}}}(s_h)} \right). \quad (15b)$$

822 Then according to the expression of $\pi(a_h|s_h)$ in (15b), we obtain the following relation:
 823

$$824 \quad \pi(a_h|s_h) \propto \pi_{\text{base}}(a_h|s_h) \exp \left(\frac{1}{\beta} A^{\pi_{\text{base}}}(s_h, a_h) \right). \quad (16)$$

826 Based on the constraint (14c), we know that $\pi(\cdot|s_h)$ is a distribution so that $\sum_{a \in \mathcal{A}} \pi(a|s_h) = 1$.
 827 Therefore, according to the expressions in (15b) and (16), we can obtain the following expression of
 828 the optimal policy π^* as below:
 829

$$830 \quad 831 \quad \pi^*(a_h|s_h) = \frac{\pi_{\text{base}}(a_h|s_h) \exp \left(\frac{1}{\beta} A^{\pi_{\text{base}}}(s_h, a_h) \right)}{\sum_{a' \in \mathcal{A}} \pi_{\text{base}}(a'|s_h) \exp \left(\frac{1}{\beta} A^{\pi_{\text{base}}}(s_h, a') \right)}.$$

834 Recall that $A^{\pi_{\text{base}}}(s_h, a_h) := Q^{\pi_{\text{base}}}(s_h, a_h) - V^{\pi_{\text{base}}}(s_h)$, then we can rewrite the expression of
 835 $\pi^*(a|s)$:
 836

$$837 \quad 838 \quad \pi^*(a_h|s_h) = \frac{\pi_{\text{base}}(a_h|s_h) \exp \left(\frac{1}{\beta} (Q^{\pi_{\text{base}}}(s_h, a_h) - V^{\pi_{\text{base}}}(s_h)) \right)}{\sum_{a' \in \mathcal{A}} \pi_{\text{base}}(a'|s_h) \exp \left(\frac{1}{\beta} (Q^{\pi_{\text{base}}}(s_h, a') - V^{\pi_{\text{base}}}(s_h)) \right)} \\ 839 \quad 840 \quad = \frac{\pi_{\text{base}}(a_h|s_h) \exp \left(\frac{1}{\beta} Q^{\pi_{\text{base}}}(s_h, a_h) \right)}{\sum_{a' \in \mathcal{A}} \pi_{\text{base}}(a'|s_h) \exp \left(\frac{1}{\beta} Q^{\pi_{\text{base}}}(s_h, a') \right)}. \quad (17)$$

845 This completes the proof. □
 846

848 B.2 PROOF OF THEOREM 1

850 Considering that the exact Q function or value function Q^{π_t} is typically unavailable in practice, it is
 851 necessary to account for the approximation error. Let \hat{Q}^{π_t} denote the estimation of Q^{π_t} at the t -th
 852 iteration via value function training step (7).

853 More specifically, $\hat{Q}^{\hat{\pi}_t}$ is defined as follows:
 854

$$855 \quad 856 \quad \hat{Q}^{\hat{\pi}_t} := \arg \min_Q \mathbb{E}_{\tau \sim \mathcal{D}_{t+1}} \left[\sum_{h=1}^H [Q(s_h, a_h) - r(\tau)]^2 \right], \quad (18)$$

858 where \mathcal{D}_{t+1} is generated by the policy $\hat{\pi}_t$.
 859

860 We assume that the estimated function also belongs to the Q function class \mathcal{F} , i.e., $\hat{Q}^{\hat{\pi}_t} \in \mathcal{F}$. The
 861 policy update then becomes:
 862

$$863 \quad \hat{\pi}_{k+1}(a|s) \propto \hat{\pi}_t(a|s) \exp(\hat{Q}^{\hat{\pi}_t}(s, a) / \beta_t). \quad (19)$$

We now decompose the performance gap between the optimal policy π^* and the current policy $\hat{\pi}_t$ as follows:

$$\begin{aligned}
 J(\pi^*) - J(\hat{\pi}_t) &\stackrel{(i)}{=} \sum_{h=1}^H \mathbb{E}_{s_h \sim d_h^{\pi^*}, a_h \sim \pi^*(\cdot|s_h)} [A^{\hat{\pi}_t}(s_h, a_h)] \\
 &\stackrel{(ii)}{=} \sum_{h=1}^H \mathbb{E}_{s_h \sim d_h^{\pi^*}} [\langle Q^{\hat{\pi}_t}(s_h, \cdot), \pi^*(\cdot|s_h) - \hat{\pi}_t(\cdot|s_h) \rangle] \\
 &= \underbrace{\sum_{h=1}^H \mathbb{E}_{s_h \sim d_h^{\pi^*}} [\langle \hat{Q}^{\hat{\pi}_t}(s_h, \cdot), \pi^*(\cdot|s_h) - \hat{\pi}_t(\cdot|s_h) \rangle]}_{:=\epsilon_1(t)} \\
 &\quad + \underbrace{\sum_{h=1}^H \mathbb{E}_{s_h \sim d_h^{\pi^*}} [\langle Q^{\hat{\pi}_t}(s_h, \cdot) - \hat{Q}^{\hat{\pi}_t}(s_h, \cdot), \pi^*(\cdot|s_h) - \hat{\pi}_t(\cdot|s_h) \rangle]}_{:=\epsilon_2(t)}, \tag{20}
 \end{aligned}$$

where step (i) uses the performance difference lemma (Lemma 1), and the step (ii) expands the advantage function as follows:

$$\begin{aligned}
 \mathbb{E}_{s_h \sim d_h^{\pi^*}, a_h \sim \pi^*(\cdot|s_h)} [A^{\hat{\pi}_t}(s_h, a_h)] &= \mathbb{E}_{s_h \sim d_h^{\pi^*}, a_h \sim \pi^*(\cdot|s_h)} [Q^{\hat{\pi}_t}(s_h, a_h) - V^{\hat{\pi}_t}(s_h)] \\
 &= \mathbb{E}_{s_h \sim d_h^{\pi^*}, a_h \sim \pi^*(\cdot|s_h)} [Q^{\hat{\pi}_t}(s_h, a_h)] - \mathbb{E}_{s_h \sim d_h^{\pi^*}} [V^{\hat{\pi}_t}(s_h)] \\
 &= \mathbb{E}_{s_h \sim d_h^{\pi^*}, a_h \sim \pi^*(\cdot|s_h)} [Q^{\hat{\pi}_t}(s_h, a_h)] - \mathbb{E}_{s_h \sim d_h^{\pi^*}, a_h \sim \hat{\pi}_t(\cdot|s_h)} [Q^{\hat{\pi}_t}(s_h, a_h)] \\
 &= \mathbb{E}_{s_h \sim d_h^{\pi^*}} [\langle Q^{\hat{\pi}_t}(s_h, \cdot), \pi^*(\cdot|s_h) - \hat{\pi}_t(\cdot|s_h) \rangle],
 \end{aligned}$$

where the first equality is by the definition of the advantage function, and the third equality follows from the fact that the value function is the expectation of Q under the corresponding policy. The first term $\epsilon_1(t)$ reflects the inherent policy suboptimality due to the iterative policy iteration, while the second term $\epsilon_2(t)$ captures the approximation error resulting from the finite-sample estimation and function approximation for the value function.

Let t_0 denote the index that minimizes the performance gap between the optimal policy π^* and the iterates $\{\hat{\pi}_t\}_{t=0}^{T-1}$, i.e., $t_0 = \arg \min_{t \in [T]} J(\pi^*) - J(\hat{\pi}_t)$, we can upper-bound the minimal performance gap as the average of performance gap of each iteration:

$$J(\pi^*) - J(\hat{\pi}_{t_0}) \leq \frac{1}{\sum_{t=0}^{T-1} 1/\beta_t} \sum_{t=0}^{T-1} \frac{1}{\beta_t} (\epsilon_1(t) + \epsilon_2(t)), \tag{21}$$

where $\epsilon_1(t)$ and $\epsilon_2(t)$ denote the policy improvement and Q-function approximation errors at iteration t , respectively, as defined in (20). The weight β_t denotes the dual variable of the KL constraints for the t -th iteration and can also be interpreted as the learning rate for iteration t .

Bounding the term $\sum_{t=0}^{T-1} \frac{1}{\beta_t} \epsilon_1(t)$

Recall the update rule in (19), the policy π_{t+1} is updated for each time step $h \in [H]$ according to

$$\hat{\pi}_{t+1}(\cdot|s_h) = \frac{\hat{\pi}_t(\cdot|s_h) \exp(\frac{1}{\beta_t} \hat{Q}^{\hat{\pi}_t}(s_h, \cdot))}{\sum_{a \in \mathcal{A}} \hat{\pi}_t(a|s_h) \exp(\frac{1}{\beta_t} \hat{Q}^{\hat{\pi}_t}(s_h, a))}, \tag{22}$$

where H denotes the episode horizon. Moreover, under Assumption 1, the estimated value function $\hat{Q}^{\hat{\pi}_t}$ is assumed to be uniformly bounded as $\|\hat{Q}^{\hat{\pi}_t}\|_\infty \leq r_{\max}$, where r_{\max} is the upper bound on the outcome reward.

Applying the Lemma 2, we obtain

$$\begin{aligned}
 \mathbb{E}_{s_h \sim d_h^{\pi^*}} \langle \hat{Q}^{\hat{\pi}_t}(s_h, \cdot), \pi^*(\cdot|s_h) - \hat{\pi}_t(\cdot|s_h) \rangle \\
 \leq \frac{r_{\max}^2}{2\beta_t} + \beta_t D_{\text{KL}}(\pi^*(\cdot|s_h) || \hat{\pi}_t(\cdot|s_h)) - \beta_t D_{\text{KL}}(\pi^*(\cdot|s_h) || \hat{\pi}_{t+1}(\cdot|s_h)). \tag{23}
 \end{aligned}$$

918 Dividing both sides of (23) by β_t yields:
919

$$\begin{aligned} 920 \quad & \frac{1}{\beta_t} \mathbb{E}_{s_h \sim d_h^{\pi^*}} \langle \hat{Q}^{\hat{\pi}_t}(s_h, \cdot), \pi^*(\cdot | s_h) - \hat{\pi}_t(\cdot | s_h) \rangle \\ 921 \quad & \leq \frac{r_{\max}^2}{2\beta_t^2} + D_{\text{KL}}(\pi^*(\cdot | s_h) || \hat{\pi}_t(\cdot | s_h)) - D_{\text{KL}}(\pi^*(\cdot | s_h) || \hat{\pi}_{t+1}(\cdot | s_h)). \end{aligned} \quad (24)$$

924 Combine (24), the weighted summation of $\epsilon_1(t)$ can be written as
925

$$\begin{aligned} 926 \quad & \sum_{t=0}^{T-1} \frac{1}{\beta_t} \epsilon_1(t) \\ 927 \quad & = \sum_{t=0}^{T-1} \frac{1}{\beta_t} \sum_{h=1}^H \mathbb{E}_{s_h \sim d_h^{\pi^*}} \langle \hat{Q}^{\pi_t}(s_h, \cdot), \pi^*(\cdot | s_h) - \hat{\pi}_t(\cdot | s_h) \rangle \\ 928 \quad & \leq \sum_{h=1}^H \mathbb{E}_{s_h \sim d_h^{\pi^*}} D_{\text{KL}}(\pi^*(\cdot | s_h) || \hat{\pi}_0(\cdot | s_h)) + \frac{r_{\max}^2 H}{2} \sum_{t=0}^{T-1} \frac{1}{\beta_t^2} \\ 929 \quad & \leq H \log(C_{\text{ST}}) + \frac{r_{\max}^2 H}{2} \sum_{t=0}^{T-1} \frac{1}{\beta_t^2}, \end{aligned} \quad (25)$$

938 where $\hat{\pi}_0 = \pi_{\text{base}}$, the first inequality applies (24), and the second inequality uses
939 the Lemma 3 by bounding the KL divergence using the concentrability constant $C_{\text{ST}} =$
940 $\max_{h \in [H], s \in \mathcal{S}_h, a \in \mathcal{A}} \frac{d_h^{\pi^*}(s, a)}{d_h^{\pi_{\text{base}}}(s, a)}$.
941

942 **Bounding the term** $\sum_{t=0}^{T-1} \frac{1}{\beta_t} \epsilon_2(t)$
943

944 The error term $\epsilon_2(t)$ is mainly caused by function approximation error in estimating the value
945 function, which is introduced by using the least-squares objective in (7) using finite samples. As the
946 intermediate rewards are zero and only the terminal reward $r(\tau)$ is assigned, the terminal reward $r(\tau)$
947 serves as an unbiased Monte Carlo estimate of the Q-value for a given state-action pair (s_h, a_h) . That
948 is

$$949 \quad Q^{\hat{\pi}_t}(s_h, a_h) = \mathbb{E}_{\tau \sim \hat{\pi}_t} \left[\sum_{i=h}^H r(s_i, a_i) | s_h, a_h \right], \quad (26)$$

950 where $\tau = (s_h, a_h, \dots, s_H, a_H)$ is a partial trajectory started from (s_h, a_h) . Thus, the relation between
951 the reward and the value function can be built as (note that $\sum_{i=h}^H r(s_i, a_i) = r(\tau)$)

$$952 \quad r(\tau) = Q^{\hat{\pi}_t}(s_h, a_h) + \varepsilon_h, \quad (27)$$

953 where the noise term $\varepsilon_h := r(\tau) - \mathbb{E}[\sum_{i=h}^H r(s_i, a_i) | s_h, a_h]$ is zero-mean conditioned on (s_h, a_h) .
954 As the \hat{Q}^{π_t} is the least square solution via
955

$$956 \quad \hat{Q}^{\hat{\pi}_t} := \arg \min_Q \mathbb{E}_{\tau \sim \mathcal{D}_{t+1}} \left[\sum_{h=1}^H [Q(s_h, a_h) - r(\tau)]^2 \right], \quad (28)$$

957 where \mathcal{D}_{t+1} is the dataset of m trajectories collected under policy $\hat{\pi}_t$.
958

959 To bound the estimation error, we apply the guarantee of least squares (Lemma 8). In particular, we
960 treat each pair (s_h, a_h) as the input u , and terminal reward $r(\tau)$ as the noisy label v . The conditional
961 distribution ρ in Lemma 8 corresponds to $d_h^{\hat{\pi}_t}$. Since $Q^{\hat{\pi}_t}(s, a) \in [-r_{\max}, r_{\max}]$ and $|r(\tau)| \leq r_{\max}$
962 and belong to the function class \mathcal{F} , all assumptions in Lemma 8 are satisfied.
963

964 Therefore, for any iteration t , with probability at $1 - \delta$, we have
965

$$966 \quad \mathbb{E}_{s \sim d_h^{\pi_1}, a \sim \hat{\pi}_0} [|\hat{Q}^{\hat{\pi}_t}(s, a) - Q^{\hat{\pi}_t}(s, a)|] \leq \sqrt{\frac{256 r_{\max}^2}{m} \log \frac{2|\mathcal{F}|}{\delta}}, \quad (29)$$

972 where m is the size of the training data, i.e., $m = |\mathcal{D}_{t+1}|$.
 973

974 To bound the error term $\sum_{t=0}^{T-1} \epsilon_2(t)/\beta_t$, we apply a union bound over $t \in [T]$, we have for all
 975 $t \in [T]$ that
 976

$$\begin{aligned}
 978 \sum_{t=0}^{T-1} \frac{1}{\beta_t} \epsilon_2(k) &= \sum_{h=1}^H \sum_{t=0}^{T-1} \frac{1}{\beta_t} \mathbb{E}_{s_h \sim d_h^{\pi^*}} \left[\langle Q^{\pi_t}(s_h, \cdot) - \hat{Q}^{\pi_t}(s_h, \cdot), \pi^*(\cdot | s_h) - \hat{\pi}_t(\cdot | s_h) \rangle \right] \\
 979 &\leq 2 \sum_{t=0}^{T-1} \frac{1}{\beta_t} \sum_{h=1}^H \left| \mathbb{E}_{s_h \sim d_h^{\pi^*}} \left[Q^{\pi_t}(s_h, \cdot) - \hat{Q}^{\pi_t}(s_h, \cdot) \right] \right| \\
 980 &\leq 2 \sum_{t=0}^{T-1} \frac{1}{\beta_t} \sum_{h=1}^H \sqrt{\mathbb{E}_{s_h \sim d_h^{\pi^*}} \left[\left| Q^{\pi_t}(s_h, \cdot) - \hat{Q}^{\pi_t}(s_h, \cdot) \right|^2 \right]} \\
 981 &\leq 2 \sum_{t=0}^{T-1} \frac{1}{\beta_t} \sum_{h=1}^H \sqrt{C_{\text{ST}} \mathbb{E}_{s_h \sim d_h^{\pi_1}} \left[\left| Q^{\pi_t}(s_h, \cdot) - \hat{Q}^{\pi_t}(s_h, \cdot) \right|^2 \right]} \\
 982 &= 2H \sqrt{C_{\text{ST}} \frac{256r_{\max}^2}{m} \log \frac{2T|\mathcal{F}|}{\delta}} \sum_{t=0}^{T-1} \frac{1}{\beta_t}, \tag{30}
 \end{aligned}$$

992 where the first inequality follows the relation $|\pi_1 - \pi_2| < 2$, the second inequality applies the
 993 Cauchy-Schwarz inequality, the third follows from Assumption 2, and the final equality uses the
 994 value function approximation bound in (29).
 995

996 In conclusion, by setting the learning rate as $\beta_t = \sqrt{t+1}/\omega$, we obtain the following bound on the
 997 performance gap with at least probability $1 - \delta$:

$$999 J(\pi^*) - J(\hat{\pi}_{t_0}) \leq \frac{H \log(C_{\text{ST}}) + r_{\max}^2 \omega^2 H \log(T)/2}{\omega \sqrt{T}} + 2H \sqrt{C_{\text{ST}} \frac{256r_{\max}^2}{m} \log \frac{2T|\mathcal{F}|}{\delta}}, \tag{31}$$

1001 where r_{\max} is the upper bound of the Q function.
 1002

1003 By choosing $\omega = \sqrt{\frac{2 \log C_{\text{ST}}}{r_{\max}^2 \log T}}$, with at least probability $1 - \delta$, we obtain
 1004

$$1005 J(\pi^*) - J(\hat{\pi}_{t_0}) \leq 2\sqrt{r_{\max}^2 H^2 \log T \log C_{\text{ST}}/T} + 2H \sqrt{C_{\text{ST}} \frac{256r_{\max}^2}{m} \log \frac{2T|\mathcal{F}|}{\delta}}. \tag{32}$$

1007 This result shows the trade-off between the number of iterations T and the number of datasets of size
 1008 m used to estimate the value function.
 1009

1010 Theorem 1 differs from Xiao (2022) in the following ways: first, the parameter β_t is a constant
 1011 or decreasing in Xiao (2022), whereas our result utilizes an adaptive increasing β_t ; second, (Xiao,
 1012 2022, Theorem 8) considers the sample-based truncation estimation error in the infinite-horizon MDP,
 1013 while we consider finite-horizon least-square value function estimation error; Third, the rate $\mathcal{O}(T^{-\frac{1}{2}})$
 1014 derived in Theorem 1 is slower than the rate of $\mathcal{O}(T^{-1})$ (under constant β_t) and the superlinear
 1015 rate (under decreasing β_t) achieved by Xiao (2022). Note that the last point is reasonable since we
 1016 are increasing the parameter β_t , which forces θ^t to stay closer to θ^{t-1} . Such a choice is practically
 1017 motivated by the LLM finetuning setting, where it is desirable that the final model is close to the base
 1018 model (which already has reasonable quality). Further, the $\mathcal{O}(T^{-\frac{1}{2}})$ rate is similar to what can be
 1019 achieved by Shani et al. (2020), which also uses increasing β_t 's. The key difference is that the latter
 1020 considers an infinite-horizon setting, while our work considers the finite-horizon setting.
 1021

1021 B.3 PROOF OF PROPOSITION 1

1022 We begin the analysis in a decision-making setting for the LLM's text generation. Considering a
 1023 deterministic, episodic, finite-horizon decision process model $(\mathcal{S}, \mathcal{A}, \mathcal{P}, r, H)$ with state space \mathcal{S} ,
 1024 action space \mathcal{A} , deterministic transition kernel \mathcal{P} , and bounded reward function r . Starting from an
 1025 initial state s_1 (prompt), the agent chooses an action from the whole action space $a_h \in \mathcal{A}$, receives a

reward $r(s_h, a_h)$, and moves to the next state s_{h+1} . Denote the entire input prompt as x and output continuation as $y := (y_1, \dots, y_H)$, where H is the maximum generation length. Thus, a complete trajectory is $\tau := (s_1, a_1, s_2, \dots, s_H, a_H)$. The optimal trajectory $\tau^* := (s_1^*, a_1^*, s_2^*, \dots, s_H^*, a_H^*)$ maximizes the cumulative reward $r(\tau) := \sum_{h=1}^H r(s_h, a_h)$. For simplicity, assume τ^* is unique. At this moment, let us keep the definition of state and actions generic.

Suppose we have access to a gold reward function r , and a sequence of value functions $\{V_i\}_{i=0}^{I-1}$ can approximate the gold value function V^* . Formally, for a trajectory $\tau = (s_1, a_1, \dots, s_H, a_H)$, these functions are given by:

$$r(\tau) = \sum_{h=1}^H r(s_h, a_h), \quad V^*(s_h) = \mathbb{E}_\tau \left[\sum_{i=h}^H r(s_i, a_i) | s_h \right]. \quad (33)$$

First, let us clarify the algorithms that we are comparing.

Algorithm 1: Best-of-N Sampling (BoN)

- 1: **Input:** Initial state s_1 , base policy π_{base} , reward model r , number of samples N , horizon H .
- 2: **Output:** Trajectory τ_{BoN} with the highest reward using BoN.
- 3: Generate N trajectories $\{\tau^1, \tau^2, \dots, \tau^N\}$ started from initial state s_1 , each with maximum horizon H
- 4: Query the reward model to compute the reward scores $r(\tau)$ for each generated trajectory $\tau \in \{\tau^1, \tau^2, \dots, \tau^N\}$
- 5: Find the trajectory τ_{BoN} with the highest reward:

$$\tau_{\text{BoN}} = \arg \max_{\tau \in \{\tau^1, \tau^2, \dots, \tau^N\}} r(\tau)$$

- 6: **return** the trajectory τ_{BoN}

Algorithm 2: Generation in IRO with I value functions

- 1: **Input:** Initial state s_1 , beam width K , successors per state B , chunk length L , value function list $\{\hat{V}_i\}_{i=0}^{I-1}$, base policy π_{base} , reward model r
- 2: **Output:** Trajectory τ_{IRO} .
- 3: Given the initial state s_1 , generate $U = KB$ partial responses with length L to initialize the candidate set $\mathcal{C} = \{\tau_1, \tau_2, \dots, \tau_U\}$
- 4: **while** $\exists \tau' \in \mathcal{C}$ such that τ' is incomplete (does not reach [EOS] token) **do**
- 5: Query the value function list $\{\hat{V}_i\}_{i=1}^I$ to compute the value scores v_j for each candidate τ_j as $v_j = \sum_{i=0}^{I-1} \frac{1}{\beta_i} \hat{V}_i(\tau_j)$.
- 6: Select the top K beams to serve as a parent set.
- 7: Generate B successors with length L for each parent node to update the candidate set \mathcal{C} .
- 8: **end while**
- 9: **return** $\tau_{\text{IRO}} = \arg \max_{\tau' \in \mathcal{C}} r(\tau')$

B.3.1 CHUNK LENGTH $L = 1$

To begin with, let us consider the case where each state and action is a single token. In this case, at each time step h , the state is defined as $s_h = [x, y_{1:h-1}]$, including the prompt x and the sequences of tokens $y_{1:h-1}$ generated up to that point. Similarly, each action $a_h = y_h$. Since each state s_h encodes a unique prefix of the output sequence up to position $h-1$, the state spaces $\{\mathcal{S}_h\}_{h=1}^H$ are mutually disjoint. The transition kernel \mathcal{P} is deterministic, i.e. given tokens $s_h = [x, y_{1:h-1}]$ and a_h , we have $s_{h+1} = \mathcal{P}(s_h, a_h) = [s_h, a_h]$. In this case, the action space \mathcal{A} is the entire vocabulary.

Given the algorithms above, we assess the computational cost of algorithms (BoN algorithm and IRO algorithm) designed to find the optimal trajectory τ^* using two key measures:

1. C_{token} : The total number of token costs, representing the number of tokens needed by the algorithm.

1080 2. C_{query} : The query cost, representing the number of calls to an external reward or value
 1081 function oracle.
 1082

1083 Specifically, BoN sampling requires N reward model evaluations to select the optimal trajectory with
 1084 the highest reward score, while IRO requires querying all I value functions at every decision step h
 1085 to select candidates.

1086 **Best-of- N algorithm.** Since actions across different time steps h are independent, the probability of
 1087 sampling the optimal trajectory τ^* is $\Pr(\tau = \tau^*) = \frac{1}{|\mathcal{A}|^H}$. Sampling N full trajectories uniformly,
 1088 the probability that at least one of them matches τ^* is:
 1089

$$1090 \Pr[\tau_{\text{BoN}} = \tau^* | N] = 1 - \left(1 - \frac{1}{|\mathcal{A}|^H}\right)^N. \quad (34)$$

1093 When $|\mathcal{A}|^H \gg N$, that is, the number of sampled trajectories is much smaller than the size of full
 1094 trajectory space, we can use $(1 - x)^n \approx 1 - nx$ for small x , and this expression can be approximated
 1095 by:
 1096

$$1097 \Pr[\tau_{\text{BoN}} = \tau^* | N] \approx \frac{N}{|\mathcal{A}|^H}. \quad (35)$$

1099 The corresponding costs can then be calculated as follows:
 1100

$$1101 C_{\text{token}}(\text{BoN}) = NH, \\ 1102 C_{\text{query}}(\text{BoN}) = N. \quad (36)$$

1104 **IRO.** Now, consider the inference of IRO with I value functions. At each step h , we uniformly
 1105 sample a subset $\mathcal{A}_h^{\text{sub}} \subset \mathcal{A}$ of a fixed size $|\mathcal{A}_h^{\text{sub}}| = U := KB$. By using value functions $\{\hat{V}_i\}_{i=1}^I$,
 1106 which can approximate the gold value function V^* (i.e., $\sum_{i=0}^{I-1} \hat{V}_i / \beta_i \approx V^*$), the algorithm selects
 1107 the action that maximizes the estimated return from this subset:
 1108

$$1109 a_h = \arg \max_{a \in \mathcal{A}_h^{\text{sub}}} V^*(s_{h+1}), \quad (37)$$

1111 where $s_{h+1} = [s_h, a]$. For the optimal action a_h^* at h -th timestep, if $a_h^* \in \mathcal{A}_h^{\text{sub}}$, then the value
 1112 functions can be used to correctly select it via (37). Since the subset $\mathcal{A}_h^{\text{sub}}$ is sampled uniformly and
 1113 independently with size U , the probability that it contains the optimal action is

$$1114 \Pr[a_h^* \in \mathcal{A}_h^{\text{sub}}] = 1 - \left(1 - \frac{1}{|\mathcal{A}|}\right)^U.$$

1117 Since each step h is independent, the probability of sampling the optimal trajectory is:
 1118

$$1119 \Pr[\tau_{\text{IRO}} = \tau^*] = \left(1 - \left(1 - \frac{1}{|\mathcal{A}|}\right)^U\right)^H \approx \left(\frac{U}{|\mathcal{A}|}\right)^H, \quad (38)$$

1121 where the approximation holds under the fact that U is much smaller than the size of vocabulary $|\mathcal{A}|$,
 1122 i.e., $|\mathcal{A}| \gg U$. Therefore, the costs of IRO are given by
 1123

$$1124 C_{\text{query}}(\text{IRO}) = UHI, \\ 1125 C_{\text{token}}(\text{IRO}) = UH. \quad (39)$$

1126 To match the success probability of the Best-of-N method, we require that the probability of (35) and
 1127 (38) are equal, i.e.,
 1128

$$1129 \left(\frac{U}{|\mathcal{A}|}\right)^H = \frac{N}{|\mathcal{A}|^H}. \quad (40)$$

1132 It follows that
 1133

$$U^H = N \Leftrightarrow U = \sqrt[H]{N}. \quad (41)$$

Now, we can compare the costs of two methods when achieving the same performance by taking the ratio between terms (36) and (39)

$$\begin{aligned} \frac{C_{\text{token}}(\text{BoN})}{C_{\text{token}}(\text{IRO})} &= \frac{NH}{UH} \stackrel{(41)}{=} \frac{U^H H}{UH} = U^{H-1}, \\ \frac{C_{\text{query}}(\text{BoN})}{C_{\text{query}}(\text{IRO})} &= \frac{N}{UHI} \stackrel{(41)}{=} \frac{U^H}{UHI} = \frac{1}{HI} U^{H-1}, \end{aligned} \quad (42)$$

B.3.2 CHUNK LENGTH $L > 1$

In the previous case, each state s_h is the generated prefix of tokens (x_1, \dots, x_{h-1}) , and each action x_h is a token from the *entire* vocabulary \mathcal{A} . That is, we consider the case where $L = 1$. In practice, choosing $L > 1$ is more efficient because fewer value function generation is needed. In this case, each a_t becomes a chunk of a token, and each s_t is still the accumulation of all the tokens generated up to time $t - 1$. The effective horizon becomes $H_c = H/L$, and the size of the action space will increase to $|\mathcal{A}|^L$.

Similarly as the analysis from the previous subsection, the probability of sampling the optimal trajectory for IRO is

$$\Pr[\tau_{\text{IRO}} = \tau^*] = \left(\frac{U}{|\mathcal{A}|^L} \right)^{H_c} = \frac{U^{H_c}}{|\mathcal{A}|^H}.$$

To ensure the sample success probability with the BoN algorithm, as shown in (35), we require that

$$\frac{U^{H_c}}{|\mathcal{A}|^H} = \frac{N}{|\mathcal{A}|^H} \quad \Leftrightarrow \quad U = \sqrt[H_c]{N}. \quad (43)$$

Therefore, by employing the chunk-level guided generation, the costs of the IRO algorithm will become

$$\begin{aligned} C_{\text{token}}(\text{IRO}) &= U \times L \times H_c = UH, \\ C_{\text{query}}(\text{IRO}) &= U \times I \times H_c = UHI/L. \end{aligned} \quad (44)$$

At this time, the ratio of the costs of two methods when achieving the same performance is

$$\begin{aligned} \frac{C_{\text{token}}(\text{BoN})}{C_{\text{token}}(\text{IRO})} &= \frac{NH}{UH} \stackrel{(43)}{=} \frac{U^{H_c} H}{UH} = U^{H/L-1} = (BK)^{H/L-1}, \\ \frac{C_{\text{query}}(\text{BoN})}{C_{\text{query}}(\text{IRO})} &= \frac{N}{UHI/L} \stackrel{(43)}{=} \frac{U^{H_c}}{UHI/L} = \frac{L}{HI} U^{H/L-1} = \frac{L}{HI} (BK)^{H/L-1}, \end{aligned} \quad (45)$$

where the last equalities for both the above relations come from the fact that, for IRO, the size of the actions being sampled at each time is given by $U = KB$. The proof is completed.

C IRO ALGORITHM

In this section, we give the algorithm flow of our proposed method IRO, which can be separated into two steps: value function training and value function guided generation.

1188
1189
1190**Algorithm 3:** The Iterative Reweight-and-Optimize (IRO) algorithm

```

1: Input: Prompt dataset  $\mathcal{D}^p := \{(x)\}$ , a base
   policy  $\pi_{\text{base}}$ , reward model  $r$ .
2: Output: Updated policy.
3: Initialize  $\hat{\pi}_0 = \pi_{\text{base}}$ ; Generate
    $\mathcal{D}_1 = \{\tau_1, r(\tau_1)\}$ , where for each  $\tau$ ,  $x \sim \mathcal{D}^p$ 
   and  $y \sim \hat{\pi}_0$ .
4: for  $t = 1$  to  $T - 1$  do
5:   Train a value function  $\hat{V}^{\hat{\pi}_{t-1}}$  by minimizing
      the objective (7) using  $\mathcal{D}^p$ .
6:   Sample a subset  $\mathcal{D}_{t+1}^p$  of size  $m$  from  $\mathcal{D}^p$ .
7:   Generate  $y_{t+1}$  with  $\hat{\pi}_t$  based on
       $x_{t+1} \in \mathcal{D}_{t+1}^p$  using value-guided generation
      (Algorithm 4) with  $\{\hat{V}^{\hat{\pi}_i}\}_{i=0}^{t-1}$ .
8:   Evaluate responses with the reward model  $r(\cdot)$ 
      to obtain  $\mathcal{D}_{t+1} := \{(\tau_{t+1}, r(\tau_{t+1}))\}$ .
9: end for
10: return  $\hat{\pi}_T$  constructed according to (8).

```

1205
1206
1207
1208
1209**Algorithm 5:** Diversity-first principle for selection of K beams

```

1: Input: Candidate set  $\mathcal{C}$ , beam width  $K$ , combined value function  $V(\cdot)$ 
2: Output: Selected beam set  $\mathcal{S}^*$ 
3: Cluster  $\mathcal{C}$  into groups via a mapping  $g : \mathcal{C} \rightarrow \mathcal{K}$ .
4: Initialize  $\mathcal{S} \leftarrow \emptyset$ , and mark all groups in  $\mathcal{K}$  as unused.
5: for  $y \in \mathcal{C}$  sorted by descending  $V(y)$  do
6:   if  $|\mathcal{S}| < K$  and group  $g(y)$  is unused then
7:     Add  $y$  to  $\mathcal{S}$  and mark group  $g(y)$  as used.
8:   end if
9: end for
10: for  $y \in \mathcal{C}$  sorted by descending  $V(y)$  do
11:   if  $|\mathcal{S}| < K$  and  $y \notin \mathcal{S}$  then
12:     Add  $y$  to  $\mathcal{S}$ .
13:   end if
14: end for
15: return  $\mathcal{S}^*$  as the final selected beam set

```

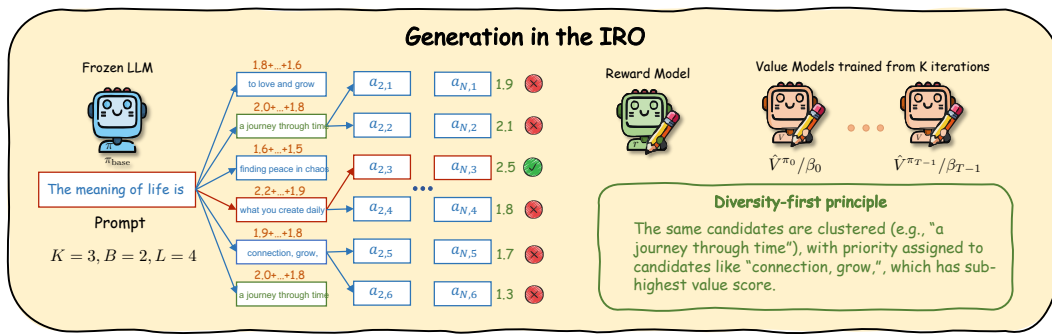
1224
1225
1226
12271238
1239
1240
1241

Figure 7: Illustration of decoding process with diversity-first principle.

Algorithm 4: Value function guided generation at the t -th iteration

```

1: Input: Prompt  $x$ , beam width  $K$ , successors
   numbers  $B$ , chunk length  $L$ , value functions
    $\{\hat{V}_i\}_{i=0}^{t-1}$ , base policy  $\pi_{\text{base}}$ , reward model  $r(\cdot)$ 
2: Output: Response  $y^*$  with the highest reward.
3: Generate  $U = KB$  partial responses with length
    $L$  to form an initial candidate set  $\mathcal{C}$ .
4: while  $\exists y' \in \mathcal{C}$  such that  $y'$  is incomplete do
5:   Compute scores for all  $\{y_j\}_{j=1}^N$  as
       $V(y_j) = \sum_{i=0}^{t-1} \frac{1}{\beta_i} \hat{V}_i(x, y_j)$ .
6:   Select top  $K$  beams with the highest value
      scores as parents.
7:   For each parent, expand  $B$  successors of
      length  $L$ , update new successors to  $\mathcal{C}$  while
      keep size as  $U$ .
8: end while
9: return  $y^* = \arg \max_{y' \in \mathcal{C}} r(x, y')$ 

```

1242 **D AUXILIARY LEMMAS**
 1243

1244 **Lemma 1** (Lemma C.4 in Chang et al. (2024)). *For any policy π and π' , the performance difference*
 1245 *can be expressed as below:*
 1246

1247
$$\eta^{\pi'}(\pi) = \sum_{h=1}^H \mathbb{E}_{s_h \sim d_h^\pi, a_h \sim \pi(\cdot|s_h)} [A^{\pi'}(s_h, a_h)] \quad (46)$$

 1248
 1249

1250 where $d_h^\pi(s) := \mathbb{E}_{s_1 \sim \mu} [\sum_{h=1}^H \mathcal{P}^\pi(s_h = s|s_1)]$ denotes the state visitation measure.
 1251

1252 **Lemma 2.** *Let $h \in [H]$ be any timestep. Assume the policy π_{t+1} is updated from π_t via:*
 1253

1254
$$\pi_{t+1}(\cdot|s_h) = \frac{\pi_t(\cdot|s_h) \exp(\frac{1}{\beta_t} f(s_h, \cdot))}{\sum_{a \in \mathcal{A}} \pi_t(a|s_h) \exp(\frac{1}{\beta_t} f(s_h, a))},$$

 1255
 1256

1257 and assume that the function f is bounded as $\|f\|_\infty \leq Q_{\max}$. Then, the following inequality holds:
 1258

1259
$$\begin{aligned} & \langle f(s_h, \cdot), \pi^*(\cdot|s_h) - \pi_t(\cdot|s_h) \rangle \\ & \leq \frac{Q_{\max}^2}{2\beta_t} + \beta_t D_{\text{KL}}(\pi^*(\cdot|s_h) || \pi_t(\cdot|s_h)) - \beta_t D_{\text{KL}}(\pi^*(\cdot|s_h) || \pi_{t+1}(\cdot|s_h)) \end{aligned} \quad (47)$$

 1260
 1261

1263 *Proof.* For convenience, we omit the state dependence s_h and use simplified notation: we write
 1264 $\pi(\cdot|s_h)$ as π and $Q(s_h, \cdot)$ as Q . For any policy p , we have
 1265

1266
$$\begin{aligned} \langle f, p - \pi_{t+1} \rangle &= \left\langle \beta_t \log \frac{\pi_{t+1}}{\pi_t} + \log Z_t, p - \pi_{t+1} \right\rangle \\ &= \left\langle \beta_t \log \frac{\pi_{t+1}}{\pi_t}, p \right\rangle + \langle \log Z_t, p \rangle - \left\langle \beta_t \log \frac{\pi_{t+1}}{\pi_t}, \pi_{t+1} \right\rangle - \langle \log Z_t, \pi_{t+1} \rangle \\ &= \beta_t \left\langle \log \frac{\pi_{t+1}}{p}, p \right\rangle + \beta_t \left\langle \log \frac{p}{\pi_t}, p \right\rangle - \beta D_{\text{KL}}(\pi_t || \pi_{t+1}) \\ &= -\beta_t D_{\text{KL}}(p || \pi_{t+1}) + \beta_t D_{\text{KL}}(p || \pi_t) - \beta_t D_{\text{KL}}(\pi_t || \pi_{t+1}). \end{aligned}$$

 1267
 1268
 1269
 1270
 1271
 1272
 1273
 1274

1275 where $Z_t = Z_t(s_h)$ is the normalization term.
 1276

1277 Thus, we have

1278
$$\begin{aligned} \langle f, p - \pi_t \rangle &= \langle f, p - \pi_{t+1} \rangle + \langle f, \pi_{t+1} - \pi_t \rangle \\ &\leq -\beta_t D_{\text{KL}}(p || \pi_{t+1}) + \beta_t D_{\text{KL}}(p || \pi_t) + \langle f, \pi_{t+1} - \pi_t \rangle \\ &\quad - \frac{\beta_t}{2} \|\pi_{t+1} - \pi_t\|_1^2 + \|Q^{\pi_t}\|_\infty \|\pi_{t+1} - \pi_t\|_1 \\ &\leq -\beta_t D_{\text{KL}}(p || \pi_{t+1}) + \beta_t D_{\text{KL}}(p || \pi_t) + \frac{\|f\|_\infty^2}{2\beta_t} \end{aligned}$$

 1279
 1280
 1281
 1282
 1283
 1284

1285 where the first inequality uses Pinsker's inequality (Lemma 5), and Hölder's inequality (Lemma 6),
 1286 and the second inequality uses the Cauchy–Schwarz inequality (Lemma 4). \square
 1287

1288 **Lemma 3** (Proposition B.5 in Chang et al. (2024)). *Let π^* denote the optimal policy and π_{base} be a
 1289 initial policy. Then the following inequality holds:*
 1290

1291
$$\sum_{h=1}^H \mathbb{E}_{s_h \sim d_h^*} D_{\text{KL}}(\pi^*(\cdot|s_h) || \pi_{\text{base}}(\cdot|s_h)) \leq H \log \left(\max_{h \in [H], s \in \mathcal{S}_h, a \in \mathcal{A}} \frac{d_h^*(s, a)}{d_h^{\pi_{\text{base}}}(s, a)} \right), \quad (48)$$

 1292
 1293

1294 where $d_h^*(s, a)$ and $d_h^{\pi_{\text{base}}}(s, a)$ denote the state-action visitation measures under π^* and π_{base} ,
 1295 respectively.

1296 *Proof.* The proof is the same as in Chang et al. (2024).
 1297

$$\begin{aligned}
 1298 \quad & \sum_{h=1}^H \mathbb{E}_{s_h \sim d_h^{\pi^*}} [D_{\text{KL}}(\pi^*(\cdot|s_h) \parallel \pi_{\text{base}}(\cdot|s_h))] = \sum_{h=1}^H \sum_{s \in \mathcal{S}_h} d_h^{\pi^*}(s) \sum_{a \in \mathcal{A}} \pi^*(a|s) \log \frac{\pi^*(a|s)}{\pi_{\text{base}}(a|s)} \\
 1299 \quad & = \sum_{h=1}^H \sum_{s \in \mathcal{S}_h, a \in \mathcal{A}} d_h^{\pi^*}(s, a) \log \frac{\pi^*(a|s)}{\pi_{\text{base}}(a|s)} \\
 1300 \quad & \leq \sum_{h=1}^H \sum_{s \in \mathcal{S}_h, a \in \mathcal{A}} d_h^{\pi^*}(s, a) \log \frac{\pi^*(a|s)}{\pi_{\text{base}}(a|s)} + \sum_{h=1}^H \sum_{s \in \mathcal{S}_h} d_h^{\pi^*}(s) \log \frac{d_h^{\pi^*}(s)}{d_h^{\pi_{\text{base}}}(s)} \\
 1301 \quad & = \sum_{h=1}^H \sum_{s \in \mathcal{S}_h, a \in \mathcal{A}} d_h^{\pi^*}(s, a) \log \frac{\pi^*(a|s)}{\pi_{\text{base}}(a|s)} + \sum_{h=1}^H \sum_{s \in \mathcal{S}_h, a \in \mathcal{A}} d_h^{\pi^*}(s, a) \log \frac{d_h^{\pi^*}(s)}{d_h^{\pi_{\text{base}}}(s)} \\
 1302 \quad & = \sum_{h=1}^H \sum_{s \in \mathcal{S}_h, a \in \mathcal{A}} d_h^{\pi^*}(s, a) \log \frac{d_h^{\pi^*}(s, a)}{d_h^{\pi_{\text{base}}}(s, a)} \\
 1303 \quad & \leq H \log \left(\max_{h \in [H], s \in \mathcal{S}_h, a \in \mathcal{A}} \frac{d_h^{\pi^*}(s, a)}{d_h^{\pi_{\text{base}}}(s, a)} \right). \\
 1304 \quad & \\
 1305 \quad & \\
 1306 \quad & \\
 1307 \quad & \\
 1308 \quad & \\
 1309 \quad & \\
 1310 \quad & \\
 1311 \quad & \\
 1312 \quad & \\
 1313 \quad & \\
 1314 \quad & \\
 1315 \quad &
 \end{aligned}$$

1316 The proof is completed. □
 1317

1318 E COMPUTATIONAL COMPLEXITY ANALYSIS

1319
 1320 In this section, we provide a comprehensive computational complexity analysis of IRO, covering both
 1321 inference time cost and the offline cost of value-function training. We first compare the inference-
 1322 time complexity of IRO with other inference-time alignment methods—such as chain-of-thought
 1323 (CoT) (Wei et al., 2022), BoN, and ARGs (Khanov et al., 2024). Secondly, we present the offline
 1324 computational cost of IRO required to train value functions and generate rollouts across iterations.
 1325

1326 **Inference-time computational complexity analysis** Assume that the total horizon is H (number
 1327 of tokens to be generated), and a beam-search-like algorithm selects K candidates and generates B
 1328 successors for each candidate, which maintains KB search width. For IRO at inference time, it uses
 1329 I value functions to guide chunk-level search with chunk length L . For a fair comparison, here we
 1330 consider $N = KB$ (where N is the # of generations used in the BoN method).
 1331

1332 In Table 1, we present a comprehensive comparison of FLOPs and latency for various methods.
 1333

- 1334 1. FLOPs: Total number of floating-point operations (e.g., additions, multiplications) executed
 1335 by the algorithm.
- 1336 2. Latency: The theoretical duration it takes an algorithm to produce a desired output, incor-
 1337 porating both compute and memory overhead. Here, it includes per-token generation and
 1338 periodic reward model calls.

1339 Since the policy model and reward model may differ in size, we separate each metric into policy and
 1340 reward. We define T_{dec} as the time to decode one token by base LLM, and T_{rm} as the time to score
 1341 by reward model or value function.

1342 Consider that the policy and reward model are both decoder-only and use KV cache, given prefix
 1343 length l , the FLOPs complexity is $O(l)$ to generate one token. Thus, CoT generates H tokens requires
 1344 $\sum_{i=1}^H O(i) = O(H^2)$ complexity. For BoN, it generates N trajectories and needs the reward model
 1345 to query N trajectories, so the FLOPs complexity is $O(NH^2)$.
 1346

1347 For the method ARGs, it requires querying the reward model to decide every token generation,
 1348 introducing high reward latency $O(HKB T_{\text{rm}})$. Our algorithm IRO uses chunk-level beam search
 1349 with chunk length L , and employs I value functions, which leads to $O(\frac{HKB}{L} T_{\text{rm}})$ reward model
 latency.

Method	FLOPs (Policy)	FLOPs (Reward)	Latency (Policy)	Latency (Reward)
CoT	$O(H^2)$	—	$O(HT_{\text{dec}})$	—
BoN	$O(NH^2)$	$O(NH^2)$	$O(HT_{\text{dec}})$	$O(NT_{\text{rm}})$
ARGS	$O(H^2KB)$	$O(H^2KB)$	$O(HT_{\text{dec}})$	$O(HKB T_{\text{rm}})$
IRO	$O(H^2KB)$	$O(H^2KBI)$	$O(HT_{\text{dec}})$	$O\left(\frac{HKB}{L}T_{\text{rm}}\right)$

Table 1: FLOPs and latency comparison for policy and reward model across different methods. Here — indicates that the method does not involve this complexity.

Offline computational complexity for IRO The offline cost of IRO consists of (1) rollout generation and (2) lightweight value-function training.

At the i -th iteration, the frozen policy is guided by $(i - 1)$ previously trained value functions. Let the rollout dataset $|\mathcal{D}| = D$, sequence length H , beam width K , and select B successors in each selection. Since the policy model and value function may differ in size, we use C_p and C_v to denote the per-token cost of the frozen policy and value function, respectively. Thus, the total rollout compute cost at iteration i is

$$O(H^2KBDC_p) + O(DH^2KB(i-1)C_v).$$

After obtaining the data, IRO trains a lightweight value function via supervised regression, which is comparable to SFT and substantially cheaper than training the full policy model.

Aggregating over I iterations, the total offline training cost is

$$O(H^2KBDIC_p) + O(DH^2KBI^2C_v),$$

plus $I - 1$ value function training cost.

F TECHNICAL LEMMAS

Lemma 4 (Cauchy-Schwarz Inequality). For $u, v \in \mathbb{R}^d$, we have

$$\langle u, v \rangle \leq \|u\| \|v\| \leq \frac{1}{2} \|u\|_2^2 + \frac{1}{2} \|v\|_2^2$$

Lemma 5 (Pinsker's inequality). For any two distributions p and q , there is always

$$D_{\text{KL}}(p\|q) \geq \frac{1}{2} \|p - q\|_1^2$$

Lemma 6 (Hölder's inequality). Let $p, q > 1$ such that $\frac{1}{p} + \frac{1}{q} = 1$. If $f \in L^p$ and $g \in L^q$, then $fg \in L^1$, and

$$\|fg\|_1 \leq \|f\|_p \cdot \|g\|_q.$$

Lemma 7 (Jensen's Inequality). Suppose that $\phi(w)$ is a convex function on Ω . Consider $w_1, \dots, w_m \in \Omega$, and non-negative numbers $\alpha_1, \dots, \alpha_m \in \mathbb{R}$ so that $\sum_{i=1}^m \alpha_i = 1$. Then,

$$\phi\left(\sum_{i=1}^m \alpha_i w_i\right) \leq \sum_{i=1}^m \alpha_i \phi(w_i).$$

Lemma 8 (Least Squares Guarantee; Lemma 15 in Song et al. (2022)). Fix any $R > 0$, $\delta \in (0, 1)$ and assume we have a class of real valued functions $\mathcal{H} : \mathcal{U} \mapsto [-R, R]$. Suppose we have K i.i.d samples $\{(u_k, v_k)\}_{k=1}^K$ where $u_k \sim \rho$ that may depend on past observations and v_k is sampled via the conditional probability $p(\cdot | u_k)$:

$$v_k \sim p(\cdot | u_k) := h^*(u_k) + \epsilon_k,$$

where $h^* \in \mathcal{H}$ and $\{\epsilon_k\}_{k=1}^K$ are independent random variables such that $\mathbb{E}[v_k | u_k] = h^*(u_k)$. Additionally, suppose that $\max_k |v_k| \leq R$ and $\max_u |h^*(u)| \leq R$. Then the least square solution $\hat{h} \leftarrow \arg \min_{h \in \mathcal{H}} \sum_{k=1}^K (h(u_k) - v_k)^2$ satisfies with probability at least $1 - \delta$,

$$\mathbb{E}_{x \sim \rho} \left[\left(\hat{h}(u) - h^*(u) \right)^2 \right] \leq \frac{256R^2 \log(2|\mathcal{H}|/\delta)}{K}.$$

The proof is the same as in Song et al. (2022) and thus is omitted here.

1404 **G GPT AS A JUDGE IN TL;DR TASK**
14051406 System Prompt in TL;DR
1407

1408 Which of the following summaries does a better job of summarizing the most important
1409 points in the given forum post, without including unimportant or irrelevant details? Judge
1410 based on accuracy, coverage, and coherence.

1411 **Post:**
1412 <post>

1413 **Summary A:**
1414 <Summary A>

1415 **Summary B:**
1416 <Summary B>

1417 FIRST provide a one-sentence comparison of the two summaries, explaining which you
1418 prefer and why. SECOND, on a new line, state only "A" or "B" to indicate your choice. Your
1419 response should use the format:

1420 **Comparison:** <one-sentence comparison and explanation>

1421 **Preferred:** <"A" or "B">

1422
1423 **H EXTENDED EXPERIMENTAL DETAILS AND RESULTS**
14241425 **H.1 TL;DR TASK**
14261427 **H.1.1 MODEL SPECIFICATION**
1428

1429 The following table lists the models and their corresponding links.
1430

1431 Models	1432 Links
1433 EleutherAI/pythia-1b SFT	vwxyzjn/EleutherAI_pythia-1b-deduped_sft_tldr
1434 EleutherAI/pythia-6.9b SFT	vwxyzjn/EleutherAI_pythia-6.9b-deduped_sft_tldr
1435 EleutherAI/pythia-1b Reward	vwxyzjn/EleutherAI_pythia-1b-deduped_reward_tldr
1436 EleutherAI/pythia-6.9b Reward	vwxyzjn/EleutherAI_pythia-6.9b-deduped_reward_tldr

1437
1438 **H.1.2 COMPUTE RESOURCES SPECIFICATION**
1439

1440 All 1B value models are trained on an A100 40G GPU. For the inference, 1B model inference takes
1441 place on one single A100 40G GPU, while 6.9b model on 2 A100 40G GPU.
1442

1443
1444 **H.1.3 GENERATION PARAMETERS**
1445

1446 We used fixed hyperparameters across all tested models. We use temperature $T = 0.7$, top-k = 50,
1447 and top-p = 1.0 with a maximum sequence length of 53 when sampling from the language model.
1448 For the beam search, we use $B = K = 4$ and $L = 16$ (B is the beam width, K is the child width,
1449 and L is the chunk length). For the BoN, we use $N = 16$ for a fair comparison.

1450
1451 **H.1.4 IMPLEMENTATION**

1452 We utilize a public reward model trained from Pythia-6.9b with TL;DR dataset as the gold
1453 evaluator to measure the quality of generated summaries.
1454

1455 For the inference-time alignment baseline, such as BoN, ARGS, and CARDS, we use the 1b reward
1456 model¹ to provide the sequential-level or token-level guidance.
1457

¹vwxyzjn/EleutherAI_pythia-1b-deduped_reward_tldr

1458 For the training-time baseline DPO, we use the public available checkpoints: the 1b model² and the
 1459 6.9b model³.
 1460

1461 For the IRO algorithm, we use $\beta_t = 1$ for all iterations. To obtain the value function, we initialize it
 1462 from the 1B reward model. In each subsequent iteration, we initialize from the value function trained
 1463 in the previous iteration. We train each value function with a learning rate 3×10^{-6} , batch size of
 1464 256, and for 10 epochs.
 1465

1466 H.1.5 ABLATION STUDY ON THE CHOICE OF β_t

1468 In this subsection, we explore the choice of parameter β_t in the TL;DR task, which controls the extent
 1469 to which the updated policy $\hat{\pi}_{t+1}$ incorporates the estimated value function $\hat{V}^{\hat{\pi}_t}$. Specifically, the
 1470 update rule is given by
 1471

$$1472 \log \hat{\pi}_{t+1}(a_h|s_h) \propto \log \hat{\pi}_t(a_h|s_h) + \hat{V}^{\hat{\pi}_t}(s_{h+1})/\beta_t,$$

1474 where $s_{h+1} = [s_h, a_h]$, and smaller values of β_t lead to more aggressive updates toward high-value
 1475 actions under $\hat{V}^{\hat{\pi}_t}$.
 1476

1477 In our implementation, we omit the term $\log \pi_t(a_h|s_h)$ when scoring the candidates, as it is already
 1478 revealed during candidate generation. In the algorithm iteration, we set $\beta_1 = 1$ for the first iteration
 1479 and perform ablations by varying β_2 for the second iteration to study its impact on performance.
 1480

1481 As shown in Fig. 8, we find that setting $\beta_2 = 1$ yields the highest performance among the values we
 1482 considered. When β_2 is increased, it places more weight on the prior policy by reducing the influence
 1483 of Q^{π_t} .
 1484

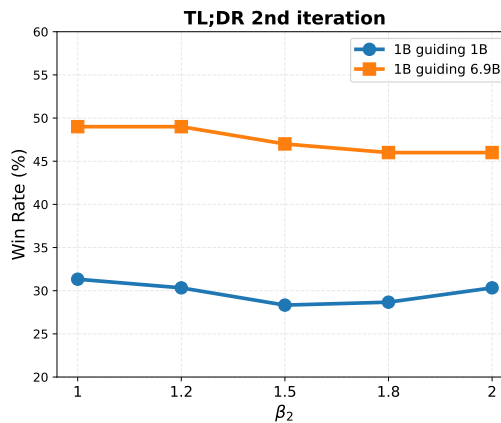


Figure 8: Ablation study on the choice of β_2 with fixed $\beta_1 = 1$. The results indicate that setting $\beta_2 = 1$ yields the highest win rate.

1502 H.2 ULTRAFEEDBACK TASK

1503 H.2.1 MODEL SPECIFICATION

1508 The following table lists the models and their corresponding links.
 1509

1510 ²[vwxyzjn/EleutherAI_pythia-1b-deduped_dpo_tldr](https://huggingface.co/vwxyzjn/EleutherAI_pythia-1b-deduped_dpo_tldr)

1511 ³[vwxyzjn/EleutherAI_pythia-6.9b-deduped_dpo_tldr](https://huggingface.co/vwxyzjn/EleutherAI_pythia-6.9b-deduped_dpo_tldr)

1512	Models	Links
1513	Meta-Llama-3-8B-Instruct	meta-llama/Meta-Llama-3-8B-Instruct
1514	Meta-Llama-3-70B-Instruct	meta-llama/Meta-Llama-3-70B-Instruct
1515	UltraFeedback dataset (Cui et al., 2023)	HuggingFaceH4/ultrafeedback_binarized
1516	sfairXC/FsfairX-LLaMA3-RM-v0.1	sfairXC/FsfairX-LLaMA3-RM-v0.1
1517	zephyr-7b-beta	HuggingFaceH4/zephyr-7b-beta
1518	mistral-7b-sft-beta	HuggingFaceH4/mistral-7b-sft-beta
1519		
1520		
1521		
1522	H.2.2 COMPUTE RESOURCES SPECIFICATION	
1523	7B value models are trained on 8 A100 40G GPU. For the inference, the 7B model inference takes	
1524	place on one 4 A100 40G GPU, while the 70b model takes place on one 4 H100 GPU.	
1525		
1526		
1527	H.2.3 HYPERPARAMETERS SPECIFICATION	
1528	We used fixed hyperparameters across all tested models. We use temperature $T = 0.6$, top-k = 50,	
1529	and top-p = 0.9 with a maximum sequence length of 2048 when sampling from the language model.	
1530	For the beam search, we use $B = K = 4$ and $L = 16$ (B is the beam width, K is the child width,	
1531	and L is the chunk length). For the BoN, we use $N = 16$ for a fair comparison.	
1532		
1533		
1534	H.2.4 IMPLEMENTATION	
1535	For the BoN with explicit reward, we trained the reward model initialized from	
1536	mistral-7b-sft-beta using RLHFlow recipe (Dong et al., 2024) with a learning rate 5×10^{-6}	
1537	and for 3 epochs.	
1538		
1539	For the implicit reward, we use the relative log probability between zephyr-7b-beta and	
1540	mistral-7b-sft-beta to calculate the implicit reward, where zephyr-7b-beta is fine-	
1541	tuned based on the mistral-7b-sft-beta using DPO loss on the Ultrafeedback dataset.	
1542	For the token-level based method ARGS and CARDS, due to the long time generation for large	
1543	maximum sequence length, we only consider ARGS due to the time limit. We use the 7b reward	
1544	model trained by ourselves to provide token-level guidance.	
1545	We don't include methods such as GenARM (Xu et al., 2024b) and IVG (Liu et al., 2024) in our	
1546	comparison, which also perform the inference time alignment, for the following reasons.	
1547		
1548	GenARM (Xu et al., 2024b) requires that the autoregressive reward model belong to the same model	
1549	family as the base model. However, their released checkpoints are based on Llama-2, while our base	
1550	model is Llama-3 family, which uses a different vocabulary size and tokenizer. In addition, in their	
1551	experiment, GenARM underperforms compared to the BoN baseline when evaluated with GPT-4	
1552	under the Alpaca Evaluation benchmark.	
1553	For IVG (Liu et al., 2024), the provided value function is trained using the prompt-continuation	
1554	evaluated by sfairXC/FsfairX-LLaMA3-RM-v0.1, which leverages extensive pairwise data,	
1555	making a direct comparison with our setup unfair. In addition, IVG's token-level implicit reward also	
1556	ties to the same model family as the base model, limiting its capability.	
1557	To train the value function in the IRO algorithm, we initialize the first iteration from the 7B reward	
1558	model. In each subsequent iteration, we initialize from the value function trained in the previous	
1559	iteration. We train each value function with a learning rate 3×10^{-6} , batch size of 512, and for 10	
1560	epochs.	
1561		
1562	H.2.5 ADDITIONAL RESULT	
1563		
1564	In this section, we present the numerical results on the Ultrafeedback task. According to both the	
1565	length control win rate and the raw win rate metrics, IRO demonstrates consistent performance	
	improvements across iterations, surpassing other baselines.	

1566	1567	Method	Compared Against GPT-4		Compared Against BoN-E	
			1568	LC Win Rate	Win Rate	LC Win Rate
1569	1570	Meta-Llama-3-8B-Instruct	30.71	29.63	38.77	38.32
1571	1572	ARGS	30.62	30.35	36.51	37.38
1573	1574	BoN-I 16	35.25	32.67	43.52	40.68
1575	1576	BoN-E 16	39.61	38.14	50.00	50.00
1577	1578	weak to strong search	36.20	35.90	44.13	42.92
1579	1580	Controlled Decoding	38.24	37.56	49.05	47.82
1581	1582	IRO Iter1	41.06	37.32	55.42	53.60
1583	1584	IRO Iter2	42.20	40.00	55.75	55.65
1585	1586	IRO Iter3	43.11	41.00	57.00	56.46
1587	1588	IRO Compressed	42.59	39.63	58.92	56.92

Table 2: AlpacaEval 2 length-controlled win rate and raw win rate compared against GPT-4. We use $\beta_1 = 1, \beta_2 = 2, \beta_3 = 2.5$, which places more emphasis on the learned value function during generation. The decoding process maintains a beam width of 4 with 4 candidates preserved per state, and $l = 16$ tokens as a state. For fairness, we use $N = 4 * 4$ for BoN.

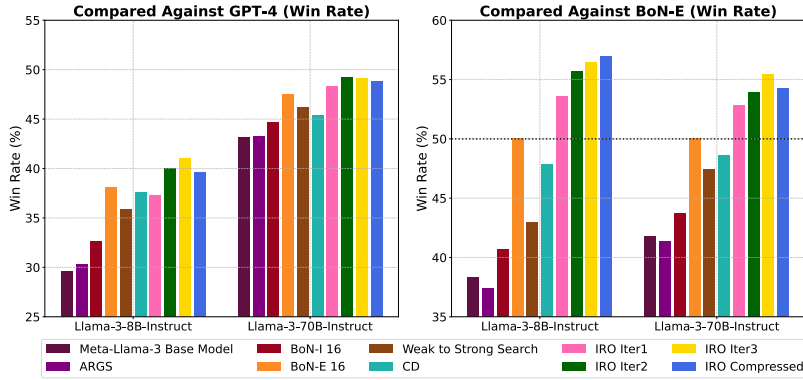


Figure 9: AlpacaEval 2 win rate compared against GPT-4 (left) and BoN-E (right) on both 7B and 70B base models, evaluated by GPT-4. We use $\beta_1 = 1, \beta_2 = 2, \beta_3 = 2.5$ while neglecting the $\log \pi(a|s)$, which places more emphasis on the learned value function during generation. The decoding process maintains a beam width of 4 with 4 candidates preserved per state, and $L = 16$ tokens as a state. For fairness, we use $N = 16$ for BoN.

1605	1606	Method	Compared Against GPT-4		Compared Against BoN-E	
			1607	LC Win Rate	Win Rate	LC Win Rate
1608	1609	Meta-Llama-3-70B-Instruct	43.11	43.11	42.39	41.80
1610	1611	ARGS	43.02	43.21	42.01	41.37
1612	1613	BoN-I 16	44.45	44.67	44.68	43.68
1614	1615	BoN-E 16	47.45	47.58	50.00	50.00
1616	1617	weak to strong search	45.37	46.21	50.00	47.45
1618	1619	Controlled Decoding	46.25	45.33	49.90	48.60
1620	1621	IRO Iter1	49.00	48.32	53.39	52.86
1622	1623	IRO Iter2	49.75	49.19	55.69	53.91
1624	1625	IRO Iter3	49.77	49.07	55.62	55.45
1626	1627	IRO Compressed	49.24	48.83	55.56	54.29

Table 3: AlpacaEval 2 length-controlled win rate and raw win rate compared against GPT-4 for 70B model. We use $\beta_1 = 1, \beta_2 = 2, \beta_3 = 2.5$. The decoding process maintains a beam width of 4 with 4 candidates preserved per state, and $l = 16$ tokens as a state. For fairness, we use $N = 4 * 4$ for BoN.

1620
1621H.2.6 ABLATION STUDY ON THE CHOICE OF β_t 1622
1623
1624
1625
1626
1627
1628

In this subsection, we explore the choice of parameter β_t in the Ultrafeedback task. Following the same experimental setup as in the TL;DR ablation, we fix $\beta_1 = 1$ for the first iteration and vary β_2 in the second iteration to analyze its effect on win rate performance. We observe that setting β_2 in the range of 1.5 to 2.0 yields the highest win rate, suggesting that this range achieves a favorable trade-off between incorporating guidance from the second-round value function and preserving information from the previous policy. These results indicate that neither overly aggressive (β_2 too small) nor overly conservative (β_2 too large) updates are optimal for effective iterative alignment.

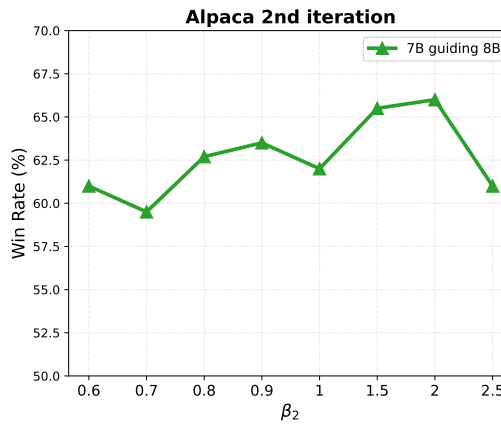
1629
1630
1631
1632
1633
1634
1635
1636
1637
1638
1639
1640
1641
1642
16431644
1645
1646
1647

Figure 10: Ablation study on the choice of β_2 with fixed $\beta_1 = 1$. The win rate is judged by GPT-4 compared against the BoN16 on the Alpaca subset. The results indicate that setting $\beta_2 = 2$ yields the highest win rate, demonstrating the sensitivity of performance to the value of β_2 .

1648
1649
1650
1651
1652
1653
1654
1655

H.3 TEST-TIME SCALING WITH VALUE FUNCTION

Here we explore how the performance of IRO scales with the search budget N across different iterations. As shown in Figure 11, the reward score evaluated using the gold reward model consistently improves with larger search budgets N , indicating that the quality of outputs generated by IRO increases accordingly.

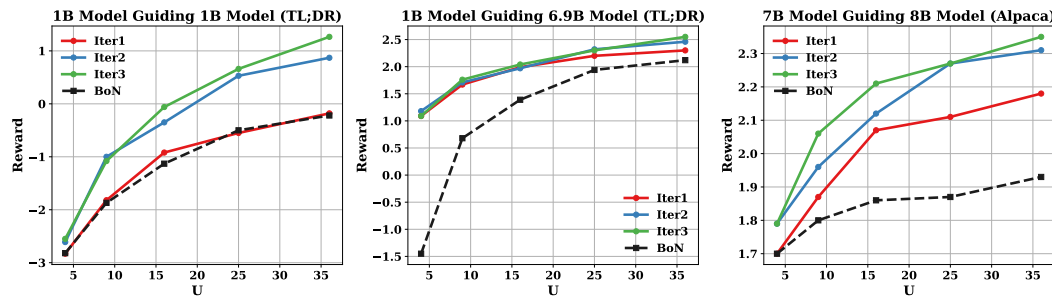
1665
1666
1667
1668

Figure 11: The reward scored by 6.9b gold reward model for TL;DR task and Alpaca subset improves with the compute budget under different iterations and BoN. During the search, we set the parameters $K = B = \sqrt{N}$.

1669
1670
1671

H.4 EXTENSION TO VERIFIABLE REWARD SETTING

1672
1673

In this section, we extended our algorithm to the verifiable reward setting, math reasoning tasks under binary reward. This demonstrates that IRO generalizes beyond continuous reward setting, such as summarization and instruction-following task.

More specifically, for verifiable rewards, we train the value function using the binary cross-entropy (BCE) loss function instead of the regression loss mentioned in (7):

$$\hat{V}^{\hat{\pi}_{t-1}} := \arg \min_V -\mathbb{E}_{\tau \sim \mathcal{D}_t} \left[\sum_{h=1}^H r(\tau) \log V(s_h) + (1 - r(\tau)) \log(1 - V(s_h)) \right], \quad (49)$$

where $r(\tau) \in \{0, 1\}$ denotes the verifiable reward, which is computed as the exact match with the ground truth label, and $V(s_h)$ denotes the prediction for state s_h .

During generation, we use the system prompt "You are a helpful assistant, and put your final answer within boxed{}." to extract the final answer. A candidate is considered correct if the boxed answer matches the ground truth.

In our experiment, we use the Qwen-3B as our frozen policy model, and 1.5B model as our value function. We evaluate the performance on a random 500 samples from the GSM8k test set (total 1318 samples) and Math500, which is a subset sampled from the dataset MATH (total 5000 samples).

We consider the following baselines: (1) majority voting, (2) train-based RL algorithm, Group Relative Policy Optimization (GRPO, (Shao et al., 2024)), and (3) Q# (Zhou et al., 2025), which trains a token-level value function to guide generation. To ensure a fair comparison, we fix the frozen base policy as Qwen-3B, and we only use the GSM8K train set for all baselines.

To implement the IRO, we generate 16 candidate completions with a temperature of 0.7 and a maximum number of new tokens of 512 for each problem. Then, we filter out all correct and incorrect questions to construct the dataset to train value functions.

Method	GSM8K (%)	Math500 (%)
Qwen-3B	44.80	21.00
Majority Voting@16	46.80	26.80
Q#	73.60	30.60
GRPO	79.80	31.80
IRO Iter1	79.61	31.50
IRO Iter2	81.27	33.40

Table 4: Comparison between baseline and IRO on math reasoning task. Here, the base model is Qwen-3B. IRO operates with $K = 4, B = 4, L = 8$, it selects the final answer as the most frequently one in the boxed answers.

From Table 4, we observe that IRO demonstrates substantial improvements on math reasoning under binary reward settings, outperforming naive majority voting by over 30% absolute on GSM8K. In addition, IRO's performance is very close to that of the RL-based method, GRPO.

These results confirm that IRO is effective not only in continuous reward setting (e.g., summarization and instruction-following), but also in binary reward settings such as math reasoning task.

H.5 ABLATION STUDY

In this subsection, we present ablation studies on the effect of chunk length L used during guided generation, and the size of the dataset used to train the value function, on the performance of IRO in its first iteration.

Explore different sampling strategies for IRO. We compare (1) beam search (Zhou et al., 2024) with and without the *diversity-first* principle, and (2) stochastic sampling methods with different temperatures. For stochastic sampling, text chunks are sampled from a softmax distribution over value scores, i.e., $a \sim \frac{\exp(V_i/T_{\text{temp}})}{\sum_j \exp V_j/T_{\text{temp}}}$. The results are shown in Fig. 12

Explore the influence of value function size in IRO To study the effect of value function size, we fix the policy and reward model while varying the value function. More specifically, on TL;DR dataset, we fix 6.9B policy and 1B reward model, and compare 1B vs. 2.8B value function sizes. On

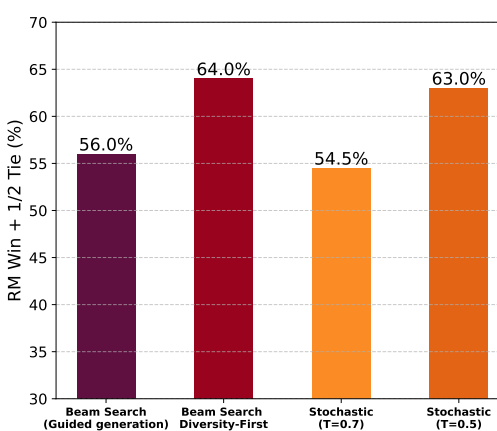


Figure 12: Beam search with the *diversity-first* principle achieves the highest win rate against the BoN baseline under various sampling strategies during the guided generation step on the 200-example subset.

Ultrafeedback dataset, we fix 8B policy and 7B reward model, and compare 2B vs. 7B value function sizes.

From Table 5 and Table 6, it is observed that larger value models (e.g., 2.8B) generally learn better and offer better guidance. Smaller ones (e.g., 2B on Ultrafeedback) may even hurt performance in some cases, even worse than naive Best-of-N.

Value Size	IRO Iter1	IRO Iter2	IRO Iter3
2.8B	36.55%	50.11%	51.78%
1B	37.66%	48.00%	49.67%

Table 5: Win rate on TL;DR task — Effect of value function size on IRO for a 6.9B policy with different value function sizes (2.8B vs 1B).

Value Size	GPT-4 LC Win Rate	BoN LC Win Rate
BoN 16	38.41	50.00
2B	37.37	38.07
7B	43.71	55.63

Table 6: Instruct-Following task - The effect of the value function size on the 1st iteration of IRO for 8B fixed policy compared against GPT-4 and BoN with $N = 16$ on a 200-sample sub-dataset.

Explore IRO’s robustness under imperfect reward models Since IRO involves using a reward model to evaluate the guided sampled data in each iteration, here we consider IRO’s robustness under an imperfect reward model on both the summarization task and the instruction following task by using different reward models of varying quality.

For the summarization task, we used three different reward models with different qualities. Here, we assume the quality of the reward model is reflected by the accuracy on two held-out test datasets, which consist of 83.8k and 2.8k pair-wise samples, respectively, shown in Table 7.

We ran IRO using 1B value functions to guide 1B and 6.9B policy models under each reward model, which is used to label and score each prompt-continuation pair during the value function training phase and select the final answer during the guided decoding phase.

From Table 8 and Table 9, despite RM 1 being weaker, IRO consistently shows performance gains over iterations. In addition, a better reward model (RM 2 or RM 3) leads to stronger improvements.

	Reward Model (RM)	Test Set 1	Test Set 2
1782	RM 1	65.81%	62.88%
1783	RM 2	68.56%	66.93%
1784	RM 3	68.74%	68.82%
1785			
1786			

Table 7: Classification accuracies on two held-out test sets for three different reward models.

IRO Iteration	RM1 Win Rate	RM2 Win Rate	RM3 Win Rate	
1791	IRO Iter1	26.00%	28.11%	28.11%
1792	IRO Iter2	31.33%	37.55%	36.00%
1793	IRO Iter3	35.33%	30.33%	37.22%

Table 8: IRO with 1B value functions guiding a 1B policy on the TL;DR dataset with different reward models. Reward scores are evaluated by a 6.9B reward model, and win rates are judged by GPT-4o against reference summaries.

IRO Iteration	RM1 Win Rate	RM2 Win Rate	RM3 Win Rate	
1800	IRO Iter1	37.66%	44.55%	40.56%
1801	IRO Iter2	48.00%	56.33%	55.00%
1802	IRO Iter3	49.67%	50.44%	51.11%

Table 9: IRO with 1B value functions guiding a 6.9B policy on the TL;DR dataset with different reward models. Reward scores are evaluated by a 6.9B reward model, and win rates are judged by GPT-4o against reference summaries.

On the Ultrafeedback dataset, we consider using a 7B value function to guide the 8B frozen policy model `LLama-3-8B-Instruct`. We tested IRO using two reward models, one trained only on the Ultrafeedback dataset and another one is a public reward model `sfairXC/FsfairX-LLaMA3-RM-v0.1`. The quality of the two reward models is measured on RewardBench, which is shown in Table 10 below.

Model	Chat	ChatHard	Safety	Reasoning	Avg
RewardModel	95.25%	58.11%	67.70%	68.26%	72.33%
sfairXC/FsfairX-LLaMA3-RM-v0.1	99.16%	64.91%	86.62%	87.16%	80.44%

Table 10: RewardBench evaluations on two reward models.

Here we only show IRO-Iter 1. We measure the performance on a 200-sample Alpaca sub-dataset, which is compared against BoN-16 and GPT-4, all of which are judged by GPT-4.

Reward Model	GPT-4 LC Win Rate	GPT-4 Raw Win Rate	BoN LC Win Rate	BoN Raw Win Rate
Reward Model	43.71	40.75	55.63	53.92
sfairXC/FsfairX-LLaMA3-RM-v0.1	47.35	45.25	54.17	55.17

Table 11: IRO Iter1 performance on a 200-sample Alpaca sub-dataset.

Overall, it is observed that by using an imperfect reward model, IRO can still achieve robust behavior and improvements. Moreover, a more accurate reward model will lead to better performance for IRO.

Explore different chunk lengths for IRO. We explore the effect of the chunk length L on the performance of IRO compared against the BoN method with $N = 16$ in the first iteration. As shown in Figure 13, performance first improves with longer chunks but then declines towards BoN as L approaches the full sequence length. Intuitively, when the chunk is too short, the value function is insufficient to distinguish the quality of different candidates. As chunk length increases, the value function can make more accurate judgments between different candidates. However, when the chunk

length approaches the full sequence, the algorithm gradually converges to the BoN method, causing the win rate relative to BoN to approach 50%. This confirms that intermediate chunk lengths best balance value-based control and sequence-level coherence.

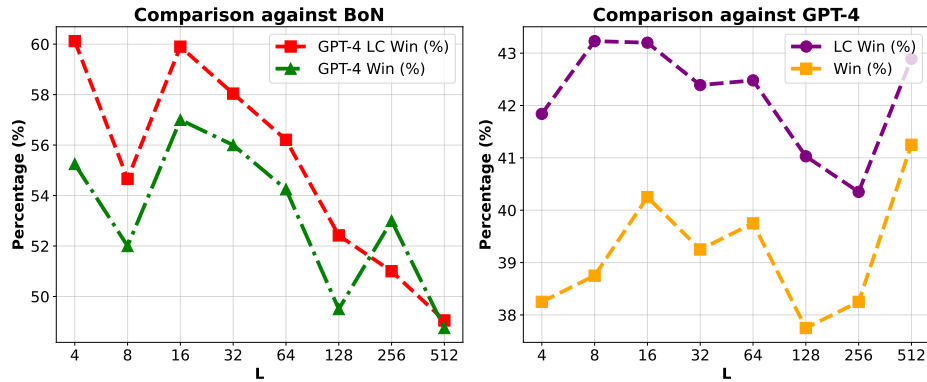


Figure 13: The effect of the chunk length on the 1st iteration of IRO compared against BoN and GPT-4 with $N = 16$ on a 200-sample sub-dataset, judged by GPT-4. Left: The comparison against BoN. Right: The comparison against GPT-4.

Explore different data sizes on training a value function for IRO. Table 12 shows the impact of data size for training a value function on the performance under different chunk length settings. When the data size is small (e.g., 1024 or 2048), larger chunk lengths ($L = 32, 64$) yield better results. This is likely because the value function trained on limited data lacks the ability to provide accurate estimates for smaller token sequences. In contrast, as data size increases (e.g., 4096 or 8192), smaller chunks ($L = 16$) perform better, suggesting that finer-grained search leads to a more accurate policy update at inference time.

Chunk Length	Data Size	GPT-4 Evaluation (%)	
		LC Win	Win
16	1024	48.61%	46.66%
	2048	51.26%	49.68%
	4096	56.45%	53.25%
	8192	59.9%	57%
32	1024	48.52%	45.51%
	2048	50.92%	51.85%
	4096	48.96%	48.75%
	8192	58.04%	56%
64	1024	53.64%	50.24%
	2048	54.63%	54.5%
	4096	53.52%	51.73%
	8192	56.21%	54.25%

Table 12: GPT-4 evaluation results on IRO-Iter1 vs. BoN-16, across different chunk lengths and value function training data sizes.

Explore different value function training. In this section, we explore several approaches to value function training, including temporal-difference (TD) learning, Generalized Advantage Estimation (GAE; Schulman et al. (2015)), and the FUDGE loss (Yang & Klein, 2021).

Let V_ϕ denote the value function parameterized by ϕ , and τ be trajectory. We summarize the loss functions for the three methods below.

1890 **TD Learning** TD learning provides a low-variance method for the value function learning. The TD
 1891 objective minimizes the squared temporal-difference error across a trajectory:
 1892

$$1893 \hat{V} := \arg \min_V \mathbb{E}_{\tau \sim \mathcal{D}_t} \left[\sum_{h=1}^H [r(s_h, a_h) + \gamma V_\phi(s_{h+1}) - V_\phi(s_h)]^2 \right]. \quad (50)$$

1896 **GAE** GAE computes a smoothed advantage estimate that interpolates between Monte Carlo returns
 1897 and TD errors, trading off bias and variance via the parameter, which is widely used in PPO algorithm.
 1898

1899 For each timestep t , the one-step TD error is:

$$1900 \delta_t = r_t + \gamma V_\phi(s_{t+1}) - V_\phi(s_t).$$

1902 The GAE advantage is computed recursively backward through the trajectory:

$$1903 \hat{A}_t = \delta_t + \gamma \lambda \hat{A}_{t+1}, \quad t = T-1, \dots, 0.$$

1905 GAE then constructs a target value for each state:

$$1906 \hat{V}_t^{\text{target}} = \hat{A}_t + V_\phi(s_t).$$

1908 which is used as a regression target for value function training. Below, we empirically show that
 1909 FUDGE loss exhibits better performance for training the token-level value function.

Method	Reward (1B guiding 1B)	Win Rate (1B guiding 1B) (%)	Reward (1B guiding 6.9B)	Win Rate (1B guiding 6.9B) (%)
SFT	-4.52	6.00	-1.33	16.33
TD $\lambda = 0.99$	-2.01	17.67	1.73	23.67
GAE $\gamma = 1, \lambda = 1$	-1.05	23.33	1.93	36.67
GAE $\gamma = 0.99, \lambda = 1$	-1.01	21.00	1.95	37.67
GAE $\gamma = 0.98, \lambda = 1$	-1.00	20.33	1.92	37.00
GAE $\gamma = 0.97, \lambda = 1$	-1.01	21.33	1.93	33.67
GAE $\gamma = 0.95, \lambda = 1$	-0.76	16.67	1.93	33.67
IRO Iter1	-0.91	26.05	1.98	37.67

1917 Table 13: Comparison between using FUDGE, TD error, and GAE for value function training on the
 1918 first iteration of IRO. Reward scores are evaluated by a 6.9B reward model, and win rates against the
 1919 reference summary are evaluated by GPT-4o-mini on 300 samples from the test dataset.

Reward Model	GPT-4 LC Win Rate	GPT-4 Raw Win Rate	BoN LC Win Rate	BoN Raw Win Rate
IRO Iter1	43.71	40.75	55.63	53.92
GAE $\gamma = 0.99, \lambda = 1$	47.35	45.25	54.17	55.17

1925 Table 14: IRO Iter1 performance on a 200-sample Alpaca sub-dataset.

I CASE STUDY

1930 Here, we display several instances from the TL;DR dataset and the Alpaca evaluation dataset. In
 1931 these cases, the response generated by our algorithm achieves successive improvement.

1932 Example 1 in the TL;DR Taks

1934 **Question** SUBREDDIT: r/loseit\n\nTITLE: Was doing great (lost 20 pounds), now worse
 1935 than ever and feel like I can't stop eating (30/f)\n\nPOST: Hello! As the title describes, I
 1936 had been losing weight (or at least maintaining) up until about two months ago. I'm now
 1937 afraid to look at the scale, but I have NOTICEABLY gained weight. Some of my clothes
 1938 don't fit me anymore. Formerly: 5'7", 160 lbs.\n\nI've been a subscriber of this site
 1939 for a long time and totally get that CICO is really the only way to lose weight, that you
 1940 shouldn't weigh yourself all that often, etc. That was never a problem before. My diet was
 1941 not incredibly strict to begin with (1 lb/week goal on MFP). I now feel like I'm straight
 1942 up addicted to food. I am eating in volumes I've NEVER eaten before. Nothing about my
 1943 life has changed beyond my eating habits.\n\nI have OCD (worried I'm compulsively

1944

eating, if that's even a thing) and bipolar 1 (yes, I am medicated; no, not with the stuff that causes weight gain – quite the opposite). I should note that I don't really feel depressed. My life is pretty decent right now! Also, I've never been a "depression eater" anyway. Oh, also, 110% sure I'm not pregnant.\n\nHow does one suppress this kind of appetite? Lately it seems that if I'm not eating, I am obsessively thinking about eating and believing I'm hungry. I can't possibly be hungry! What can I do to get back to eating a normal, reasonable amount that would result in gradual weight loss (last I checked, my TDEE was something like 2,000 but I've gained weight since then...)? I have NEVER been an overeater before; any weight gain in the past has been due to eating a moderate amount of complete shit, not eating LOTS of complete shit. I don't even know how to go about losing weight when my issue is the volume I'm eating and not the nutrition (or lack thereof).\n\nTL;DR:

1945

1946

1947

1948

1949

1950

1951

1952

1953

1954

1955

1956

Reference

Developed an issue with overeating and constantly feeling hungry. This has never been the case with me before, so I have no clue as to how to attack weight loss from a volume standpoint and not just a nutrition standpoint.

Reward Score 3.08

1960

1961

1962

1B Base

Eating 2-4 meals a day, having gained weight and feeling like I can't stop eating without reaching the point of insanity, and feeling depressed and OCD.\n\n*How to get my weight back where it needs to be?\n\n*How to

Reward Score -4.91

1963

1964

1965

1B BoN 16

I'm stuck with an abnormally high volume of food even though I'm in control of my eating behavior. Help? #f5\n\nTL;DR: My eating behavior, though low volume, high variability, and obsessive (

Reward Score -0.36

1966

1967

1B ARGs

I'm a "depression eater" (depressed/bipolar 1/OCD/depressed/eating compulsively/depressed/eating compulsively/depressed/eating compulsively/depressed/eating compulsively/b

Reward Score -1.89

1968

1969

1B CARDS

I'm obsessively thinking about eating, I have no appetite, I'm getting fatter. How can I stop?\n\nTL;DR: Obsessively thinking about eating, I have no appetite, I'm getting fatter. How can I stop?

Reward Score 0.42

1970

1971

1B Guiding 1B Iter1

Lost 20 pounds, gained 20 pounds, feel like I can't stop eating and my life has become miserable, don't know how to get back to eating a normal, reasonable amount of food.\n\nTL;DR: Lost 20 pounds, gained 20

Reward Score -3.28

1972

1973

1B Guiding 1B Iter2

Lost 20 pounds, gained 20 pounds, gained 10 pounds the past two months and feel like I'm addicted to food and can't control it... \n\nGot the title, thanks for your input! \n\nTL

Reward Score -1.10

1974

1975

1B Guiding 1B Iter3

1998
 1999 I've gained weight and am worried I'm addicted to food. I've never been an overeater
 2000 and want to lose weight, and need advice on how to get back to eating like I used to, not
 2001 obsessively thinking about eating.\n\n
 2002 **Reward Score** 1.64

2003
 2004 **6.9B Base**
 2005 Eating 2,000 calories a day without any exercise, and feeling like I am eating more than I
 2006 ever have before. Want to lose weight, but I'm not sure how and I'm not sure how to cope.
 2007 \nI also have a reddit
 2008 **Reward Score** -4.88

2009
 2010
 2011 **6.9B BoN 16**
 2012 Was losing weight. Loseit helped, but now, after years of being an underweight girl on
 2013 a steady diet (even when I was working out/eating well!), can't stop eating. I may be an
 2014 addict...
 2015 **Reward Score** 2.30

2016
 2017 **6.9B ARGS**
 2018 Gained 30 lbs, now I'm 30 lbs heavier and feel like I can't stop eating (lots of complete shit).
 2019 I'm not depressed, just a compulsive eater..
 2020 **Reward Score** 0.17

2021
 2022 **6.9B CARDS**
 2023 I'm 30/f and ate a lot, and now gained weight. Now I want to lose weight, but am afraid I'll
 2024 never be able to eat again...
 2025 **Reward Score** -0.89

2026
 2027 **1B Guiding 6.9B Iter1**
 2028 Was doing great. Gained weight, worse than I've ever been, and I can't stop eating. How do I
 2029 go about eating less to drop the weight?....
 2030 **Reward Score** 2.83

2031
 2032 **1B Guiding 6.9B Iter2**
 2033 Was doing great. Gained weight, feel like I can't stop eating. How do I regain control of my
 2034 eating?.....
 2035 **Reward Score** 3.20

2036
 2037 **1B Guiding 6.9B Iter3**
 2038 Was doing well losing weight, now in worse shape than ever and feel the need to eat even
 2039 more. How can I get back to eating a moderate amount of healthy food and losing weight?\n
 2040 **Reward Score** 4.44

2041 Example 2 in the TL;DR Taks
 2042
 2043
 2044
 2045
 2046
 2047
 2048

2049 **Question** SUBREDDIT: r/dating_advice\n\nTITLE: Not even sure if this is the right
 2050 place for this... but I think I might be confused about my sexuality? [24F]\n\nPOST:
 2051 I was raised Catholic, and even though I'm not religious anymore, I definitely still deal

2052
 2053 with the Catholic guilt. I also think I have body dysmorphic disorder, as I feel extremely
 2054 self-conscious about my body (even though my ex assured me that I have nothing to be
 2055 ashamed of, that I'm very sexy, etc.)\n\nOk so here's the part I'm confused about: guys
 2056 that I think are pretty cute and interesting to talk to, whenever it gets to the point where
 2057 I should probably kiss them or make some other kind of physical move, I shut down and
 2058 do nothing. In that moment I find myself doubting whether or not I am actually attracted
 2059 to them or something? It's like the anxiety of taking it to the next level overrides all the
 2060 other emotions. \n\nAlso it's this weird thing where I've never really learned to "flirt"
 2061 and I think that a lot of my interactions with guys tend to skew towards friendliness rather
 2062 than... flirting or whatever? So then that's like an added layer of awkwardness where there's
 2063 this platonic exchange going on but we're supposed to suddenly get "sexy" or whatever.
 2064 \n\nI didn't have a huge sex drive with my ex. He pretty much wanted it every day,
 2065 whereas I was closer to once every week or two. At the beginning of our relationship I
 2066 wanted it more often. We had pretty great sex overall, at least when I was sincerely in
 2067 the mood. \n\nDoes any of this seem to indicate that I'm not heterosexual?\n\nTL;DR:
 2068

2069 **Reference**

2070 I find myself having sort of platonic relationships with men even when I find them attractive.
 2071 Hard to initiate the sexual stuff, not sure if it's insecurity/Catholic guilt or cuz I'm not straight.

2072 **Reward Score** 2.45

2073 **1B Base**

2074 This whole "sexuality" discussion makes me so very uncomfortable! What do? It's really
 2075 driving me nuts if so...?\n\n*Sorry if something doesn't make sense*\n\n*Why would I
 2076 think about sex, or how would that be

2077 **Reward Score** -5.53

2078 **1B BoN 16**

2079 Not sure if I'm just asexual or if I'm in denial about being attracted to other people. When I
 2080 flirt with guys I kind of shut down because I have anxiety that they are somehow into me or
 2081 it's like they aren't my real friends and

2082 **Reward Score** -3.56

2083 **1B ARGS**

2084 I'm not sure if I'm a lesbian or bisexual, and I'm not sure if I'm attracted to
 2085 guys.\n\n*sigh*\n\nTL;DR: I'm not sure if I'm a lesbian or bisexual, and

2086 **Reward Score** -5.47

2087 **1B CARDS**

2088 I don't know how to deal with my body image issues or body dysmorphic disorder. I'm not
 2089 sure if I'm straight, and I don't want to be.\n\nTL;DR: I don't know how to deal with my
 2090 body image issues or body dysmorphic disorder. I'm not sure if I'm straight, and I don't want
 2091 to be.

2092 **Reward Score** -2.23

2093 **1B Guiding 1B Iter1**

2094 Was raised Catholic, have body dysmorphic disorder, am confused as to whether or not I am
 2095 attracted to guys, and if so, how to deal with the issue.\n\nocalypse!\n\nTL;DR: I was
 2096 raised Catholic,

2097 **Reward Score** -3.65

2098 **1B Guiding 1B Iter2**

2099 I find myself doubting whether or not I'm attracted to guys that I think are "pretty cute" or
 2100 "interesting to talk to" whenever it gets to the point where I should kiss them or make some
 2101 other kind of physical move.\n\n

2102 **Reward Score** 0.98

2106

2107

2108

2109

2110

2111

2112

2113

2114

2115

2116

2117

2118

2119

2120

2121

2122

2123

2124

2125

2126

2127

2128

2129

2130

2131

2132

2133

2134

2135

2136

2137

2138

2139

2140

2141

2142

2143

2144

2145

2146

2147

2148

2149

2150

2151

2152

2153

2154

2155

2156

2157

2158

2159

1B Guiding 1B Iter3

I find myself doubting whether or not I'm sexually attracted to guys who I think are cute and interesting. I don't know if I'm just being paranoid and insecure, or if my body dysmorphic disorder is holding me back or something.\n

Reward Score 2.83

6.9B Base

Am a very self conscious person. It's so bad that if men want to talk to me in a non-friendlier environment I shut down and do nothing... or feel like I might be attracted to them? —

Reward Score -3.52

6.9B BoN 16

not sure if I'm bi or gay, always feel anxious about hooking up, I have no idea how/if I should bring it up to anyone I might be interested in.

Reward Score 1.36

6.9B ARGs

Guys I'm interested in tend to be "cute" and "cuddly" and I'm not sure if I'm actually attracted to them.

Reward Score -2.95

6.9B CARDS

Guys I think are cute and interesting to talk to, and I want to kiss them but then I can't do it.

Reward Score -1.66

1B Guiding 6.9B Iter1

Catholic guilt, body dysmorphic, and self-consciousness lead to me not even trying to initiate anything with a guy I find cute and interesting.

Reward Score 1.27

1B Guiding 6.9B Iter2

I have body dysmorphia and am pretty self-conscious about my body. I find myself doing certain actions in situations where I think I should be flirting but am not, and I'm wondering if this is a sign that I'm gay?

Reward Score 1.39

1B Guiding 6.9B Iter3

I feel like a lot of my interactions with guys are very friendly and not at all sexual. I have body dysmorphic disorder and I'm not sure if I'm actually attracted to guys, and am also not sure if I'm bisexual or something.

Reward Score 2.20

2160
2161

Example 1 in the Instruct Following Task

2162
2163**Question** My friend's dog just died and they're really sad. How do I comfort them?

2164

8B Base

I'm so sorry to hear that your friend is going through a tough time. Losing a pet is never easy. Here are some ways you can comfort your friend:
 1. Listen: Allow your friend to express their emotions and thoughts without interrupting or judging. Sometimes, people just need someone to listen to them without offering solutions.
 2. Validate their feelings: Let your friend know that their feelings are normal and that it's okay to feel sad, angry, or overwhelmed. You can say something like, "I'm so sorry to hear about the loss of your furry friend. It's completely normal to feel sad and grieving."
 3. Offer physical comfort: A hug, a pat on the back, or a gentle touch on the arm can be comforting. However, make sure to respect your friend's boundaries if they don't want physical contact.
 4. Share a memory: If you have a fond memory of the dog, share it with your friend. This can help them feel less alone in their grief and bring a smile to their face.
 5. Avoid clichés: Phrases like "It was just a dog" or "You can always get another one" can come across as insensitive. Instead, focus on the emotional bond your friend had with their pet.
 6. Help with practical tasks: Offer to help your friend with tasks like cleaning, cooking, or running errands. This can take some burden off their plate and give them more time to focus on their grief.
 7. Respect their boundaries: Everyone grieves differently, and some people may need more time and space than others. Respect your friend's boundaries and don't push them to talk or do things they're not ready for.
 8. Encourage self-care: Suggest healthy coping mechanisms like exercise, meditation, or spending time in nature. Encourage your friend to take care of themselves during this difficult time.
 9. Offer to go with them: If your friend wants to visit the dog's grave, go with them. Having someone to accompany them can make the experience less overwhelming.
 10. Be patient: Grief is a process, and it's okay if your friend takes time to work through their emotions. Be patient and understanding, and let them know that you're there for them whenever they need you.

Some additional tips:
 * Avoid saying "It's just a dog" or "You can always get another one." These phrases can come across as insensitive and dismissive of your friend's feelings.
 * Don't try to "fix" the situation or offer a solution. Grief is a process, and there's no quick fix.
 * Avoid comparing your friend's grief to that of someone who has lost a human loved one. Each person's grief is unique, and it's important to respect that.
 * Consider sending a card, flowers, or a memorial gift to show your support and condolences.

Remember, the most important thing you can do is be present and supportive for your friend during this difficult time.

2165

Reward Score

3.22

2166

2167

2168

2169

2170

2171

2172

2173

2174

2175

2176

2177

2178

2179

2180

2181

2182

2183

2184

2185

2186

2187

2188

2189

2190

2191

2192

2193

2194

2195

2196

Reward Score

3.22

8B BoN-E 16

I'm so sorry to hear that your friend is going through a tough time. Losing a beloved pet is never easy. Here are some ways you can comfort your friend:
 1. Listen and validate their feelings: Allow your friend to express their emotions without judgment. Let them know that their feelings are normal and that it's okay to feel sad, angry, or overwhelmed.
 2. Offer physical comfort: A hug, a pat on the back, or a gentle touch on the arm can be comforting. Physical contact can help release oxytocin, the "cuddle hormone," which can reduce stress and anxiety.
 3. Share fond memories: Ask your friend to share stories about their dog, and listen attentively. Share your own fond memories of the dog, if you have any. This can help your friend feel less alone and more connected to their pet.
 4. Avoid clichés: Phrases like "It was just a dog" or "They're in a better place" can come across as insensitive. Instead, focus on the dog's importance in your friend's life and acknowledge the depth of their grief.
 5. Respect their boundaries: Everyone grieves differently, and some people may not want to talk about their feelings or share memories. Respect your friend's boundaries and give them space if that's what they need.
 6. Offer practical help: Help your friend with tasks such as cleaning, laundry, or errands. This can take some burden off their plate and give them more time to focus on their grief.
 7. Suggest a memorial or ritual: If your friend is comfortable with it, suggest doing something to honor their dog's memory, such as planting a tree, making a donation to an animal welfare organization, or creating a memory box.
 8. Be patient:

2211

2212

2213

2214

2215

2216

2217

2218

2219

2220

2221

2222

2223

2224

2225

2226

2227

2228

2229

2230

2231

2232

2233

2234

2235

2236

2237

2238

2239

2240

2241

2242

2243

2244

2245

2246

2247

2248

2249

2250

2251

2252

2253

2254

2255

2256

2257

2258

2259

2260

2261

2262

2263

2264

2265

2266

2267

Grief is a process, and it may take time for your friend to work through their emotions. Be patient and understanding, and let them know that you're there for them whenever they need you.\n9. Encourage self-care: Losing a pet can be physically and emotionally exhausting. Encourage your friend to take care of themselves by getting enough sleep, eating well, and engaging in activities that bring them comfort and joy.\n10. Remind them of their strength: Losing a pet can be a significant blow, but it's also a testament to your friend's capacity for love and compassion. Let them know that they're strong and capable of getting through this difficult time.\n\nRemember, there's no one-size-fits-all approach to comforting someone who's lost a pet. Be genuine, empathetic, and patient, and let your friend know that you're there to support them.

Reward Score 4.25

Weak to Strong Search (7B Guiding 8B)

I'm so sorry to hear that your friend is going through this. Losing a beloved pet can be a devastating experience. Here are some ways you can comfort your friend:\n\n1. Listen and validate their feelings: Allow your friend to express their emotions without judgment. Let them know that their feelings are normal and that it's okay to grieve the loss of their pet.\n2. Be present: Sometimes, physical presence can be comforting. Sit with your friend, hold their hand, or give them a hug. Let them know that you're there for them.\n3. Share fond memories: Share stories and memories of the dog with your friend. This can help them feel better and remember the good times they had with their pet.\n4. Avoid clichés: Phrases like "It was just a dog" or "They're in a better place" can come across as insensitive. Instead, focus on acknowledging your friend's feelings and the importance of their pet in their life.\n5. Offer practical help: Help your friend with tasks such as cleaning up after the pet, taking care of other pets in the household, or running errands. This can take some of the burden off their plate and give them more time to grieve.\n6. Respect their boundaries: Everyone grieves differently, and some people may need more time and space than others. Respect your friend's boundaries and don't push them to talk or share more than they're comfortable with.\n7. Encourage self-care: Losing a pet can be physically and emotionally draining. Encourage your friend to take care of themselves by getting enough rest, eating well, and engaging in activities that bring them comfort and relaxation.\n8. Consider a memorial or ritual: Some people find it helpful to create a memorial or ritual to honor their pet. This could be something as simple as lighting a candle, planting a tree, or creating a memory book.\n9. Be patient: Grief is a process, and it can take time for your friend to come to terms with their loss. Be patient and understanding, and let them know that you're there for them in the long haul.\n10. Remind them that they're not alone: Losing a pet can be a isolating experience, but it's important for your friend to know that they're not alone. Remind them that you're there for them, and that many people have gone through a similar experience.\n\nRemember, everyone grieves differently, and there's no one-size-fits-all approach to comforting your friend. The most important thing you can do is be present, supportive, and understanding.

Reward Score 3.65

7B Guiding 8B Iter1

I'm so sorry to hear that your friend is going through this tough time. Losing a beloved pet is never easy. Here are some ways you can comfort your friend:\n\n1. Listen: Allow your friend to express their emotions and thoughts without interrupting or judging. Listen actively and show empathy through your body language and tone of voice.\n2. Validate their feelings: Acknowledge that their feelings are normal and valid. Let them know that it's okay to feel sad, angry, or overwhelmed.\n3. Share a memory: Share a fond memory of their dog, if you have one. This can help your friend feel comforted and reminded of the good times they shared with their pet.\n4. Offer physical comfort: Sometimes, physical touch can be comforting. Offer a hug, hold their hand, or give them a gentle pat on the back.\n5. Help with practical tasks: Offer to help with tasks such as cleaning, cooking, or running errands. This can help take some of the burden off your friend and give them more time to grieve.\n6. Respect their boundaries: Everyone grieves differently, and it's essential to respect your friend's boundaries. If they don't want to talk or don't feel like being around

2268
2269
2270
2271
2272
2273
2274
2275
2276
2277
2278
2279
2280
2281
2282
2283

people, give them space.\n7. Encourage self-care: Suggest healthy coping mechanisms like exercise, meditation, or spending time in nature. Encourage your friend to take care of themselves physically and emotionally.\n8. Be patient: Grieving is a process that takes time. Be patient and understanding, and avoid putting pressure on your friend to "get over it" or "move on."\n9. Offer a memorial idea: Suggest a memorial idea, such as planting a tree, creating a memory box, or making a donation to an animal welfare organization in their dog's name.\n10. Check in regularly: Check in with your friend regularly to show that you're thinking of them and care about their well-being.\n\nSome specific phrases you could use to comfort your friend include:\n\n* "I'm so sorry to hear about the loss of your dog. My heart goes out to you."
* "You're not alone in your grief. I'm here for you, and I'll support you through this tough time."
* "Remember all the good times you had with your dog? Those memories will always be with you."
* "It's okay to feel sad, angry, or overwhelmed. Those are all normal emotions when we lose someone we love."
\n\nRemember to be genuine and sincere in your condolences, and your friend will appreciate your support during this difficult time.

Reward Score 3.89

2284
2285
2286
2287
2288
2289
2290
2291
2292
2293
2294
2295
2296
2297
2298
2299
2300
2301
2302
2303
2304
2305
2306
2307
2308
2309
2310
2311
2312
2313

7B Guiding 8B Iter2

I'm so sorry to hear that your friend is going through a tough time. Losing a beloved pet can be incredibly painful. Here are some ways you can comfort your friend:\n\n1. Listen actively: Allow your friend to express their emotions and thoughts without interrupting or judging. Listen attentively to what they're saying, and show empathy through your words and body language.\n2. Validate their feelings: Acknowledge the pain and sadness your friend is feeling. Let them know that it's okay to feel this way and that their emotions are valid. You can say something like, "I'm so sorry to hear about the loss of your dog. It's normal to feel sad and grieving."\n3. Offer physical comfort: Sometimes, physical touch can be comforting. Hold your friend's hand, give them a hug, or offer a gentle touch on the arm or shoulder. However, respect their boundaries and only offer physical comfort if they seem open to it.\n4. Share memories: If your friend is comfortable with it, share some fond memories of their dog. This can help them feel less alone in their grief and provide a sense of comfort and nostalgia.\n5. Help with practical tasks: Losing a pet can be overwhelming, and your friend may not have the energy or motivation to take care of practical tasks. Offer to help with things like cleaning, errands, or meal preparation.\n6. Respect their boundaries: Everyone grieves differently, and it's essential to respect your friend's boundaries and pace. Don't push them to talk or share more than they're comfortable with, and avoid minimizing their feelings or telling them to "get over it."\n7. Suggest a memorial or ritual: Creating a memorial or ritual can be a meaningful way to honor your friend's pet and help them process their grief. This could be something simple like lighting a candle, planting a tree, or creating a memory box.\n8. Be patient: Grief is a process that takes time, and it's essential to be patient with your friend. Avoid putting pressure on them to "move on" or "get over" their loss.\n9. Encourage self-care: Losing a pet can be emotionally and physically draining. Encourage your friend to take care of themselves by getting enough rest, eating well, and engaging in activities that bring them comfort and joy.\n10. Follow up: Check in with your friend regularly to show that you're still thinking of them and care about their well-being. This can help them feel less isolated and more supported during this difficult time.\n\nRemember, there's no one-size-fits-all approach to comforting someone who's lost a pet. The most important thing is to be present, empathetic, and understanding.

Reward Score 3.91

2314
2315
2316
2317
2318
2319
2320
2321

7B Guiding 8B Iter3

I'm so sorry to hear that your friend is going through this difficult time. Losing a beloved pet can be a devastating experience. Here are some ways you can comfort your friend:\n\n1. Listen actively: Allow your friend to express their emotions and thoughts without interrupting or judging. Listen attentively to their stories, memories, and feelings about their dog.\n2. Validate their emotions: Acknowledge your friend's pain and let them know that their feelings are normal. You can say something like, "I'm so sorry you're going through this. It's okay to feel sad, angry, or overwhelmed."\n3. Offer physical comfort: Sometimes, physical

2322
 2323 touch can be comforting. Offer a hug, hold their hand, or give them a gentle pat on the
 2324 back. However, respect their boundaries if they don't feel like physical contact.\n4. Share
 2325 memories: Share fond memories of the dog or stories about your own pets. This can help
 2326 your friend feel less alone and more connected to others who have experienced a similar
 2327 loss.\n5. Avoid clich  es: Phrases like "It was just a dog" or "They're in a better place"
 2328 can come across as insensitive. Instead, focus on acknowledging your friend's grief and
 2329 offering support.\n6. Help with practical tasks: Offer to help with tasks such as cleaning
 2330 up the dog's area, taking care of other pets, or running errands. This can help take some
 2331 burden off your friend's plate and give them more time to grieve.\n7. Respect their grief
 2332 timeline: Everyone grieves at their own pace, and there's no set timeline for mourning.
 2333 Respect your friend's emotional state and don't pressure them to "get over it" or "move
 2334 on."\n8. Encourage self-care: Suggest healthy coping mechanisms like exercise, meditation,
 2335 or spending time in nature. Encourage your friend to take care of themselves physically and
 2336 emotionally.\n9. Be patient: Losing a pet can be a long and difficult process. Be patient
 2337 with your friend and remember that it may take time for them to heal.\n10. Consider a
 2338 memorial or ritual: Suggest doing something to honor the dog's memory, such as planting
 2339 a tree, making a donation to an animal welfare organization, or creating a memory book.
 2340 This can help your friend feel more connected to their pet and find closure.\n\nRemember,
 2341 everyone grieves differently, and there's no one-size-fits-all approach to comforting your
 2342 friend. Be present, empathetic, and understanding, and let your friend know that you're there
 2343 for them during this difficult time.

Reward Score 4.41

2344
 2345
 2346
 2347
 2348
 2349
 2350
 2351
 2352
 2353
 2354
 2355
 2356
 2357
 2358
 2359
 2360
 2361
 2362
 2363
 2364
 2365
 2366
 2367
 2368
 2369
 2370
 2371
 2372
 2373
 2374
 2375

70B Base

I'm so sorry to hear that your friend is going through a tough time. Losing a pet is never easy, and it's wonderful that you want to be there for them. Here are some tips on how to comfort your friend:\n\n1. **Listen and validate their feelings**: Allow your friend to express their emotions without judgment. Let them know that their feelings are normal and that it's okay to feel sad, angry, or guilty. Validate their loss by acknowledging the significance of their pet in their life.\n2. **Offer physical comfort**: A gentle hug, a comforting touch, or a sympathetic ear can go a long way in providing comfort. Sometimes, physical touch can be more comforting than words.\n3. **Let them talk**: Encourage your friend to share stories and memories of their pet. This can help them process their grief and celebrate the good times they had with their furry friend.\n4. **Avoid clich  es**: Phrases like "It was just a pet" or "You can always get another one" can come across as insensitive. Instead, focus on the unique bond your friend shared with their pet.\n5. **Respect their boundaries**: Everyone grieves differently, and it's essential to respect your friend's boundaries. If they don't feel like talking, that's okay. Let them know you're there for them when they're ready to talk or need company.\n6. **Offer practical help**: Help your friend with tasks like making arrangements for the pet's remains, taking care of other pets in the household, or running errands. This can help take some burden off their plate.\n7. **Share a fond memory**: If you have a fond memory of their pet, share it with your friend. This can help them feel comforted knowing that others also cared about their pet.\n8. **Encourage self-care**: Grief can be exhausting. Encourage your friend to take care of themselves, whether it's getting enough rest, eating well, or engaging in activities they enjoy.\n9. **Be patient**: Grieving is a process that takes time. Be patient and understanding, and let your friend know that you're there for them in the long haul.\n10. **Remember important dates**: Mark important dates like the anniversary of their pet's passing or their pet's birthday. Reach out to your friend on these days to show you're still thinking of them and their beloved pet.\n\nSome specific things you could say to comfort your friend include:\n\n* "I'm so sorry for your loss. My heart goes out to you."
 * "Your pet was such an important part of your life, and it's okay to feel sad."
 * "I'm here for you, and I'll support you through this tough time."
 * "Do you want to talk about your pet? I'm all ears."
 * "Remember all the good times you had with your pet? Those memories will always be with you."
 \n\nRemember, there's no one-size-fits-all approach to comforting a grieving friend. Be genuine, empathetic, and patient, and you'll be helping your friend navigate this difficult

2376

2377

2378

2379

2380

2381

time.

Reward Score 5.25**70B BoN-E 16**

I'm so sorry to hear that your friend is going through a tough time. Losing a pet is never easy, and it's wonderful that you want to be there for them. Here are some tips on how to comfort your friend:\n\n1. **Listen and validate their feelings**: Allow your friend to express their emotions without judgment. Let them know that their feelings are normal and that it's okay to feel sad, angry, or guilty. Acknowledge the significance of their loss and the bond they shared with their dog.\n2. **Offer physical comfort**: A hug, a pat on the back, or a gentle touch on the arm can go a long way in providing comfort. Sometimes, physical touch can be more comforting than words.\n3. **Let them talk about their pet**: Encourage your friend to share stories, memories, and anecdotes about their dog. This can help them process their grief and celebrate their pet's life.\n4. **Avoid clichés**: Phrases like "It was just a dog" or "You can always get another pet" can come across as insensitive. Instead, focus on the unique bond your friend shared with their dog and the impact it had on their life.\n5. **Be present**: Spend time with your friend, even if it's just sitting together in silence. Your presence can be comforting and help them feel less alone.\n6. **Respect their boundaries**: Everyone grieves differently, and it's essential to respect your friend's boundaries and needs. If they don't feel like talking, that's okay. Let them know you're there for them when they're ready to talk or need support.\n7. **Offer practical help**: Depending on your friend's needs, you could offer to help with tasks like cleaning, cooking, or running errands. This can help take some burden off their plate and give them more time to focus on their grief.\n8. **Encourage self-care**: Suggest activities that can help your friend relax and cope with their emotions, such as going for a walk, practicing yoga, or engaging in a hobby they enjoy.\n9. **Remember important dates**: Mark the anniversary of their dog's passing or their birthday, and reach out to your friend on those days to show you're still thinking of them and their pet.\n10. **Be patient**: Grieving is a process that takes time, and it's essential to be patient and understanding. Avoid putting pressure on your friend to "get over it" or "move on" too quickly.\n\nRemember, there's no one-size-fits-all approach to comforting a friend who's lost a pet. Be genuine, empathetic, and supportive, and you'll be helping your friend navigate this difficult time.

Reward Score 5.5**Weak to Strong Search (7B Guiding 70B)**

I'm so sorry to hear that your friend is going through a tough time. Losing a pet is never easy, and it's essential to be supportive and understanding during this difficult period. Here are some tips to help you comfort your friend:\n\n1. **Listen and validate their feelings**: Allow your friend to express their emotions without judgment. Let them know that their feelings are normal and that it's okay to feel sad, angry, or guilty. Validate their grief by acknowledging the significance of their pet's role in their life.\n2. **Offer physical comfort**: A gentle hug, a pat on the back, or a comforting touch on the arm can go a long way in providing comfort. Physical touch can help release oxytocin, a hormone that promotes feelings of calmness and bonding.\n3. **Let them talk about their pet**: Encourage your friend to share stories, memories, and anecdotes about their dog. This can help them process their grief and celebrate the life of their beloved pet.\n4. **Avoid clichés and platitudes**: Phrases like "It was just a dog," "You can always get another pet," or "Time heals all wounds" can come across as insensitive and dismissive. Instead, focus on expressing empathy and understanding.\n5. **Respect their boundaries**: Everyone grieves differently, and it's essential to respect your friend's boundaries and needs. If they don't feel like talking, that's okay. Let them know you're there for them when they're ready to open up.\n6. **Offer practical help**: Help your friend with tasks such as making arrangements for the pet's remains, taking care of other pets in the household, or running errands. This can help take some burden off their plate and give them more time to focus on their emotional well-being.\n7. **Encourage self-care**: Suggest activities that can help your friend relax

2430

and cope with their grief, such as going for a walk, practicing yoga, or engaging in a hobby they enjoy.\n8. ****Remind them of the good times**:** Share fond memories of their dog and highlight the happy times they shared. This can help your friend focus on the positive aspects of their pet's life and find comfort in those memories.\n9. ****Be patient**:** Grief is a process that takes time, and it's essential to be patient and understanding. Let your friend know that you're there for them in the long haul, not just in the immediate aftermath of their pet's passing.\n10. ****Check in regularly**:** After the initial shock has passed, it's essential to continue checking in with your friend regularly. This can help them feel supported and remembered during a difficult time.\n\nRemember, there's no one-size-fits-all approach to comforting a friend who's lost a pet. Be genuine, empathetic, and understanding, and you'll be well on your way to providing the support they need.

2441

Reward Score 5.68

2442

2443

2444

7B Guiding 70B Iter1

2445

2446

2447

2448

2449

2450

2451

2452

2453

2454

2455

2456

2457

2458

2459

2460

2461

2462

2463

2464

2465

2466

2467

2468

2469

2470

2471

2472

2473

2474

I'm so sorry to hear that your friend is going through a tough time. Losing a pet is never easy, and it's wonderful that you want to be there for them. Here are some tips on how to comfort your friend:\n\n1. ****Listen and validate their feelings**:** Allow your friend to express their emotions without judgment. Let them know that it's okay to feel sad, angry, or guilty, and that their feelings are valid. Listen attentively to what they say, and show empathy through your body language and tone of voice.\n2. ****Acknowledge the loss**:** Recognize the significance of the loss and acknowledge the bond between your friend and their pet. You can say something like, "I'm so sorry about the loss of your furry friend. I know how much they meant to you."\n3. ****Share a fond memory (if you have one)**:** If you have a fond memory of their pet, share it with your friend. This can help them remember happy times and feel comforted. For example, "I'll never forget when [pet's name] did [funny/cute thing]. They were such a character!"\n4. ****Offer physical comfort**:** Sometimes, physical touch can be comforting. Offer a hug, hold their hand, or give them a gentle pat on the back. Be mindful of personal boundaries, though, and respect their space if they don't want physical contact.\n5. ****Avoid cliché's**:** Phrases like "It was just a pet" or "You can always get another one" can come across as insensitive. Avoid minimizing their loss or implying that their pet was replaceable.\n6. ****Be present**:** Spend time with your friend, even if it's just sitting together in silence. Your presence can provide comfort and let them know they're not alone.\n7. ****Help with practical tasks**:** Offer to help with tasks like making funeral arrangements, taking care of other pets, or doing errands. This can help take some burden off their plate and give them more time to grieve.\n8. ****Respect their boundaries**:** Everyone grieves differently, and it's essential to respect your friend's boundaries and needs. If they don't want to talk or need some alone time, give it to them.\n9. ****Check in regularly**:** Losing a pet can be a long and difficult process. Check in with your friend regularly to show you care and are thinking of them.\n10. ****Encourage self-care**:** Grief can be exhausting. Encourage your friend to take care of themselves, whether it's getting enough rest, eating well, or engaging in activities they enjoy.\n\nRemember, there's no one-size-fits-all approach to comforting a friend who's lost a pet. Be patient, understanding, and flexible, and let your friend know that you're there for them.

Reward Score 5.19

2475

2476

2477

2478

2479

2480

2481

2482

2483

7B Guiding 70B Iter2

I'm so sorry to hear that your friend is going through a tough time. Losing a pet is never easy, and it's wonderful that you want to be there for them. Here are some tips on how to comfort your friend:\n\n1. ****Listen and validate their feelings**:** Allow your friend to express their emotions without judgment. Let them know that it's okay to feel sad, angry, or guilty, and that their feelings are normal. Validate their grief by acknowledging the significance of their loss.\n2. ****Offer physical comfort**:** Sometimes, a gentle hug, a pat on the back, or a comforting touch on the arm can go a long way in providing comfort. Be mindful of your friend's personal space, but a gentle physical gesture can help them feel less alone.\n3. ****Let them talk about their pet**:** Encourage your friend to share stories, memories, and

2484

2485

2486

2487

2488

2489

2490

2491

2492

2493

2494

2495

2496

2497

2498

2499

2500

2501

2502

2503

2504

2505

2506

2507

2508 anecdotes about their dog. This can help them process their grief and celebrate the life of
 2509 their beloved pet.\n4. ****Avoid clich\u00e9s and platitudes**:** Phrases like "It was just a
 2510 dog" or "You can always get another pet" can come across as insensitive. Instead, focus
 2511 on expressing empathy and understanding.\n5. ****Respect their boundaries**:** Everyone
 2512 grieves differently, and it's essential to respect your friend's boundaries and needs. If they
 2513 don't feel like talking, don't push them. Let them know you're there for them when they're
 2514 ready to open up.\n6. ****Offer practical support**:** Help your friend with practical tasks,
 2515 such as making arrangements for the pet's remains, cooking a meal, or running errands. This
 2516 can help take some burden off their plate and give them time to focus on their grief.\n7.
 2517 ****Share a fond memory (if you have one)**:** If you have a fond memory of their dog, share it
 2518 with your friend. This can help them feel comforted knowing that others also cared about
 2519 their pet.\n8. ****Encourage self-care**:** Grief can be exhausting. Encourage your friend
 2520 to take care of themselves, whether it's getting enough rest, eating well, or engaging in
 2521 activities that bring them comfort and relaxation.\n9. ****Be patient**:** Grief is a process
 2522 that takes time, and it's essential to be patient and understanding. Let your friend know that
 2523 you're there for the long haul and that you'll support them through this difficult time.\n10.
 2524 ****Remind them of their strength**:** Losing a pet can make your friend feel vulnerable and
 2525 weak. Gently remind them of their strength and resilience, and let them know that they
 2526 can get through this tough time.\n\nRemember, there's no one-size-fits-all approach to
 2527 comforting a friend who's lost a pet. Be genuine, empathetic, and patient, and let your friend
 2528 know that you're there to support them every step of the way.

2529 **Reward Score** 5.53

7B Guiding 70B Iter3

2530

2531

2532

2533

2534

2535

2536

2537

2538

2539

2540

2541

2542

2543

2544

2545

2546

2547

2548

2549

2550

2551

2552

2553

2554

2555

2556

2557

2558

2559

2560

2561

2562

2563

2564

I'm so sorry to hear that your friend is going through a tough time. Losing a pet can be
 2509 incredibly painful, and it's wonderful that you want to be there for them. Here are some tips
 2510 to help you comfort your friend:\n\n1. ****Listen and validate their feelings**:** Allow your
 2511 friend to express their emotions without judgment. Let them know that their feelings are
 2512 normal and that it's okay to feel sad, angry, or guilty. Validate their pain by acknowledging
 2513 the significance of their loss.\n2. ****Offer physical comfort**:** Sometimes, a gentle hug, a
 2514 hand on the shoulder, or a comforting touch can go a long way in providing comfort. Be
 2515 mindful of your friend's boundaries, but a physical gesture can help them feel supported.\n3.
 2516 ****Let them talk about their pet**:** Encourage your friend to share stories, memories, and
 2517 anecdotes about their dog. This can help them process their grief and celebrate their pet's life.
 2518 Listen attentively and show interest in what they're sharing.\n4. ****Avoid clich\u00e9s**:** Phrases like "It was just a pet" or "You can always get another dog" can come across as
 2519 insensitive. Avoid minimizing their loss or implying that their feelings are not justified.
 2520 Instead, focus on the unique bond they shared with their pet.\n5. ****Respect their grieving
 2521 process**:** Everyone grieves differently, and there's no set timeline for healing. Be patient
 2522 and understanding, and let your friend know that you're there for them in the days, weeks, or
 2523 months ahead.\n6. ****Offer practical help**:** Depending on your friend's needs, you could
 2524 offer to help with errands, cook meals, or assist with tasks that might be overwhelming them.
 2525 This can help take some burden off their plate and give them space to focus on their grief.\n7.
 2526 ****Create a memorial or ritual**:** Suggest doing something to honor their pet's memory,
 2527 like lighting a candle, planting a tree, or creating a memorial photo album. This can help
 2528 your friend feel more connected to their pet and find closure.\n8. ****Remind them of happy
 2529 times**:** Share fond memories of their dog or encourage your friend to do so. Focusing on
 2530 the happy times can help balance out the sadness and provide some comfort.\n9. ****Be
 2531 present**:** Sometimes, simply being present with your friend can be incredibly comforting.
 2532 Sit with them, go for a walk, or engage in a quiet activity together. Your presence can help
 2533 them feel less alone in their grief.\n10. ****Check in regularly**:** After the initial shock of
 2534 the loss has passed, it's essential to continue checking in with your friend regularly. Grief can
 2535 be a long and winding road, and your ongoing support can make a significant difference in
 2536 their healing process.\n\nRemember, there's no one-size-fits-all approach to comforting a
 2537 friend who's lost a pet. Be patient, understanding, and flexible, and let your friend guide you
 2538 on how best to support them during this difficult time.

2538

2539

2540

2541

2542

2543

Reward Score 6.0

2544

J THE USE OF LARGE LANGUAGE MODELS

2545

In this work, large language models (LLMs), such as GPT-5, were only used as a writing assistant. It includes using GPT-5 to help with writing, such as grammar checking, word refinement, and improving readability.

2546

2547

2548

2549

2550

2551

2552

2553

2554

2555

2556

2557

2558

2559

2560

2561

2562

2563

2564

2565

2566

2567

2568

2569

2570

2571

2572

2573

2574

2575

2576

2577

2578

2579

2580

2581

2582

2583

2584

2585

2586

2587

2588

2589

2590

2591